Sensitivity Analysis of large Rotor Diameter on Offshore Wind Turbines with Suction Foundation

Øystein Sunde Thomassen

Project description

Objective

This study includes a review of technical solutions for large offshore wind turbines. Special consideration is to be made on rotor blade design as the diameter increases. Learn how to utilize FEDEM Windpower to analyze offshore wind turbines with wind and wave load cases. FEDEM shall be used to analyze interaction frequencies with turbine and waves. Main purpose of the thesis is to perform a sensitivity analysis on the second bending mode as the rotor diameter increases. Identify if there is a limit to the rotor diameter considering the second bending mode of the system.

Scope of work

- Technology review on large offshore wind turbines.

- Learn to utilize FEDEM windpower to analyze offshore wind turbines. Special consideration is to be made on interaction frequencies and bending modes.

- Analyze interaction frequency ranges of turbine and waves.

- Sensitivity analysis on second bending mode with increasing rotor diameter.

The work scope may prove to be larger than initially anticipated. Subject to approval from the supervisors, topics may be deleted from the list above or reduced in extent.

In the thesis the candidate shall present his personal contribution to the resolution of problems within the scope of the thesis work

Theories and conclusions should be based on mathematical derivations and/or logic reasoning identifying the various steps in the deduction.

Ownership

NTNU has according to the present rules the ownership of the thesis. Any use of the thesis has to be approved by NTNU (or external partner when this applies). The department has the right to use the thesis as if the work was carried out by a NTNU employee, if nothing else has been agreed in advance.

Thesis supervisors

Jørgen R. Krokstad (principal research engineer – professor II)

Abstract

This thesis has an objective aimed at understanding the sensitivity of the support structure for an offshore wind turbine with bucket foundation as the turbines get larger. The focus has been on the response and forces on turbine blades in turbulent wind and how these responses propagates to the foundation of the structure. Special attention is given to the second global bending modes of the support structure. The response in the connection between the bucket and transition piece is simulated for several load cases of wind and waves. The simulations are for wind speeds in operational mode and not extreme wind where the turbine is shut down.

The response and forces in the bucket are important to understand. Especially for being able to assess the fatigue life of the structure. Waves and wind have a wide range of frequencies, but the energy is mostly in the lower frequencies below the first natural frequency of the structure. The turbine blades will on the other hand have peaks in force and response in the rotational frequency of the rotor and its higher harmonic frequencies when calculated in a rotational sampling. They may propagate to the foundation and contribute to response around the second global bending mode of the structure.

To investigate the response in the bucket, simulations were performed in Fedem Windpower. Fedem windpower provides a powerful simulation tool for dynamic analysis of complete wind turbine systems. Three-dimensional wind field were created in TURB-SIM. Wind field based on IEC Kaimal spectrum with a turbulence intensity of 18% were created. Fully integrated coupled simulations with wind and waves where performed. AeroDyn is used for reading the wind files and calculate the forces on the turbine blades. Fedem Windpower uses the loads calculated by AeroDyn as input to its dynamic solver. Waves calculated from the JONSWAP spectrum was used in the simulations.

The results indicates that there will be response in the foundation due to waves and wind. Both wave and wind will contribute to response around the first natural frequency of the structure. Waves in form of wave excitation around the natural frequency of the structure and wind in form of the rotating blades. The effect of rotating blades will also create response around the second natural frequency of the structure. This means that both waves and wind have to be carefully considered when assessing fatigue damage to the structure.

Sammendrag

Denne avhandlingen har som mål å forstå følsomheten til støttestrukturen til en offshore vindturbin med bøttefundament når turbinene blir større. Fokuset har vært på respons of krefter på turbinbladene i turbulent vind og hvordan responsen propagerer viderer til fundamentet av strukturen. Spesiell oppmerksomhet er gitt til de globale bøyemodene til strukturen. Responsen i festet mellom overgangsstykket og bøtten er simulert for flere lasttilfeller. Simuleringne er for vindhastigheter hvor turbinen produserer strøm og ikke i ekstemvind hvor turbinen er stengt av.

Responsen og kreftene i fundamentet er viktig å forstå. Spesielt for å være i stand til å vurdere utmattingslevetiden av strukturen. Bølger og vind har en vid rekke av frekvenser, men energien er for det meste i de lave frekvensene under første egenfrekvena av strukturen. Turbinbladene vil på den andre siden ha topper i krefter og respons rundt rotasjonsfrekvensen til rotoren of dens høyere harmoniske frekvenser når de blir beregnet i rotasjonsdomenet. Responsen kan propagere til fundamentet og bidra til respons rundt andre bøyemode av strukturen.

For å undersøke responsen i bøtten ble det gjennomført simuleringer i Fedem Windpower. Fedem tilbyr et kraftig analyseverktøy for dynamisk analyse av komplette vindturbinsystemer. Tredimensjonale vindfelt ble laget i TURBSIM. Vindfelt basert på IEC Kaimal spekter med turbulensintensitet på 18% ble laget. Fullintegrert koblede simuleringer med bølger og vind ble gjennomført. AeroDyn blir brukt for å lese vindfilene å beregne kraften på turbinbladene. Fedem Windpower bruker lastene bergnet av AeroDyn som input til sin egen dynamiske simulering. Bølger som blir beregnet utifra JONSWAP spectrumet ble brukt i simuleringene.

Resultatene indikerer at det vil være respons i fundamentet på grunn av bølger og vind. Både bølger og vind vil bidra til respons rundt den føste egenfrekvensen til structuren. Bølger i form av bølgeeksitasjon rundt den første egenfrekvensen av strukturen, og vind i form av rotasjonen til bladene. Effecten av roterende blader vil også skape respons rundt den andre egenfrekvensen til strukturen. Dette betyr at både bølger og vind må bli tatt i betraktning når man anslår utmattingsskadene på strukturen.

Acknowledgement

This thesis is based on my M.Sc. study in the Department of Marine Technology at the Norwegian University of Science and Technology, with specialization in Marine Hydrodynamics. This project with the topic of Sensitivity Analysis of Offshore Wind Turbines with Suction Foundation, is performed as part of my Master degree in Marine Technology.

I would like to express my sincere gratitude towards my supervisor, Jørgen Ranum Krokstad, Principal Research Engineer Offshore Wind, Statkraft and Adjunct Professor, NTNU. He gave me the opportunity to write my project thesis and continue with my Master thesis within offshore wind. He has helped me define a very interesting thesis and guided me through most of my problems. He has given me new input and another point of view on theory and results. Without his help, this thesis would have been much smaller and less interesting than it turned out to be.

Special thanks to Lene Eliassen, Research Engineer Offshore Wind, NTNU. She has been helping me with everything from problems in the model, simulation and theory. This thesis would not have been possible without her help.

Also a big thanks to my fellow students Tine Trøen and Øivind Paulshus. Both who have been available for discussion and help during the thesis work. I would also like to thank FEDEM technology who have provided FEDEM Windpower for this thesis and given a course on how to use the software.

Finally I would like to thanks my fellow students at my office for a great last year at Marine Technology, NTNU.

Øystein Sunde Thomassen

Trondheim, June 10, 2014

Contents

List of Figures

List of Tables

1 Introduction

1.1 Background

Wind energy has been utilized as a power source for centuries. Windmills was originally used to grind corn and pump water. Today, wind energy is commonly associated with production of electricity from wind turbines. Due to the sufficient supply of sheep energy from fossil fuel and nuclear plants, the technology development in wind turbines has been relatively slow. However, the increasing focus on climate change and the fact that oil is a limited resource has given a new focus on renewable energy. Governments are giving more subsidies and companies are using more resources on renewable energy.

Wind power is considered a promising solution for meeting the increasing demand for energy. There has been a great development in onshore wind turbines, and several land-based wind farms has been installed over the world. Still, there are environmental and technological challenges for onshore wind farms. They may inflict a great impact on the surrounding environment and may cause concern to neighbouring citizens due to view and noise. Land based transport opportunities also gives a limitation on the size of the turbines.
Offshore wind turbines has less potential to affect the surrounding environment. Better wind speeds are available offshore compared to on land, which will result in higher contribution in terms of electricity supplied per turbine. Transportation on sea gives an opportunity for greater dimensions to the turbines since they can be transported by ships.

Offshore wind turbines has great potential. Still there are economical and technological challenges that needs to be solved. Large wind turbines will increase the production per unit installed and make it more economically attractive to invest. The forces on the turbine and foundation will increase with larger rotor diameter. Natural frequencies and fatigue damage is of major concern for the turbine and foundation. Ultimate stresses may also be a concern for large wind turbines.

1.2 Motivation and objective

As the turbines becomes larger, the dynamic behaviour of the structure becomes an important issue. Larger turbines may be installed in deeper waters. As a consequence the length of the tower will increase. The length of the tower have to be further increased when the blades gets longer to have enough clearance to the sea surface. According to simple beam theory, the increase of beam length will result in more flexibility to the beam. This will cause larger response of the structure if it is not properly stiffened. Longer blades will cause greater forces and response in the blades when subjected to turbulent wind. Larger response in the blades may propagate to other parts of the structure. Compared with offshore oil and gas platforms, an offshore wind turbine will experience much larger wind forces due its large blades. As a consequence there will be

much larger horizontal forces and moment in the foundation.

The objective of this thesis is to study the dynamic response of the blades in operational mode and see how they propagate to the foundation. The second bending mode of the structure is of special interest as the response of the blades have peaks at higher frequencies than the environmental loads which the turbine is subjected to.
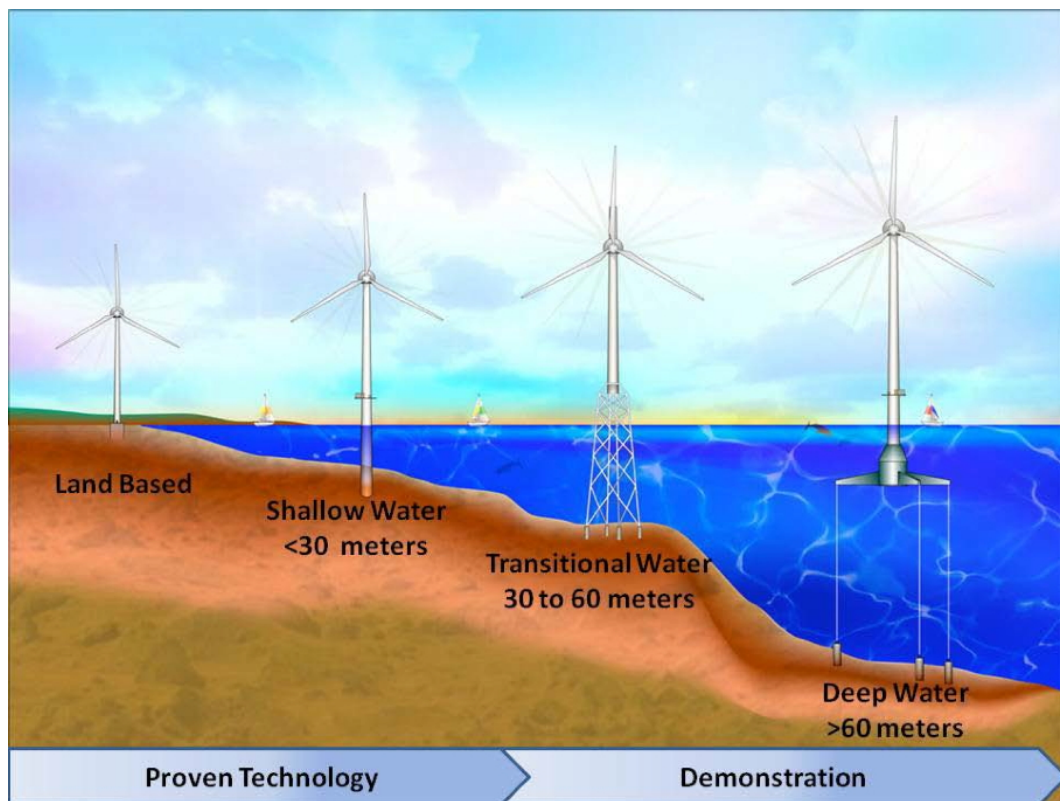
Figure 1-3. Status of offshore wind energy technology

Figure 1.1: Deep water wind turbine development (Source: National Renewable Energy Laboratory)

1.3 Thesis outline

The thesis starts with describing why we want to build larger turbines and some criteria for larger blade in Section 1. It is followed up by a description of the bucket foundation in section 2. It describes which forces a bucket needs to overcome as a foundation for offshore wind turbines.

In Section 4, Stochastic and random processes are described. It describes how Fourier Transformation is used to describe waves and how we can transform a time series into the frequency domain with use of Fast Fourier Transform.

The following sections describes the environmental loads which the turbine is subjected to. Section 5 describes waves and Section 6 describes the wind. Statistical characteristics of the loads are presented.

Dynamics are essential for offshore wind turbines. Section 7 describes basics of dynamics and dynamic considerations for the structure. The eigen-value calculation which is used to find natural frequencies of the structure is presented. Chapter 8 describes natural frequency considerations for an offshore wind turbine.

The model description is presented in chapter 9. The dimensions of the model and main characteristics of the turbine is describes. Properties of soil model is also presented.

Chapter 10 to 14 describes the simulations performed during the thesis. Eigen-value analysis, constant wind analysis and fully integrated coupled simulations with wind and waves are given. The set-up and load cases for the simulations is described.

Finally there is the conclusion and further work in Section 15 and 16.

1.4 Software used

The following computer programs were used to complete this thesis:

- FEDEM Windpower, commercial software for wind turbine design. Used to perform fully integrated wind and waves analysis on turbine model. Fedem Technology.

- TURBSIM, A stochastic, full field, turbulent-wind simulator, NREL.

- MATLAB, high-level interactive environment for numerical computation, visualization and programming. MathWorks Inc.

2 Large offshore wind turbines

2.1 Why build larger turbines?

The cost of building offshore wind turbines is very high. Companies are depending on subsidies to develop and make investment for offshore wind farms. The main purpose of technical development is to reduce the cost per kilowatt hour produced. One important factor for the price per kWh is how much electricity a turbine can produce during a year. This is again dependent on the wind conditions in the area. One of the reasons for developing larger wind turbines is to be able to utilize lower wind speeds so that the availability of the turbine is increased.

2.2 Large Turbine Blades

Increasing turbine blades introduce new challenges for wind turbines. High stiffness, low density in material and good fatigue performance are important considerations in wind turbine blade design [2].

- High material stiffness is needed to maintain optimal aerodynamic performance.

- Low density is needed to reduce gravity forces.

- Long-fatigue life is needed to reduce material degradation.

The deflection of the blades increase approximately with the cube of the blade length [11]. The deflection of the blades makes the stiffness of the blades an increasingly important factor. The stiffness will ensure that the blades does not collide with the tower for ultimate limit wind conditions. It is also important that the blades keep the shape of the aerodynamic profile. Another important factor for blades is the weight of the blades. The weight of the the blades will locally influence the inertia and gravity loads on the blades. Globally it will influence the gravity and inertia loads on the tower as well as influence the eigenfrequencies of the whole structure. Brønsted illustrates how the weight of the blade increases with the length of the blades [2]. Figure 2.1 plots the weight of different manufactures versus blade length. The trend line indicates that the weight increases with an exponent of about 2.6. This is considerably lower than the expected exponent of 3 from simple theory. The figure also shows three recent blades with length of 54 to 61.5 meters with further improvement as they are below the extrapolated empirical curve. This shows that the manufacturers are able to improve the weight for longer blades.
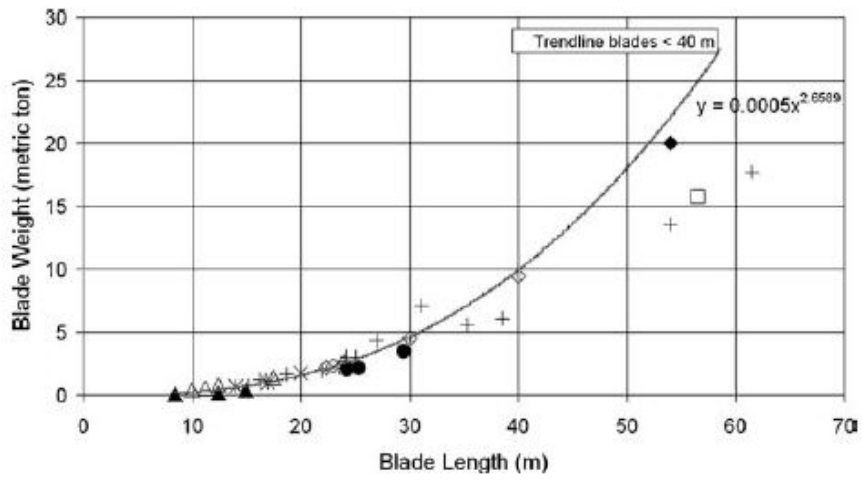
Figure 2.1: Development in rotor blade weight versus length [2]

3 Bucket foundation

The bucket foundation has shown positive results as foundation for offshore wind turbines. The steel weight of the foundation can be reduced by up to half compared with a traditional monopile solution. The installation is easier and does not require the same heavy lifting equipment as traditional foundations. As one of the main concerns for offshore wind turbine is the cost, the bucket foundation may contribute to lower investment cost.

3.1 Bucket foundation compared to suction caisson

The bucket foundation for offshore wind turbines differs in the mode of operation from a suction caisson known from traditional offshore structures like platforms on jackets [12]. Suction caisson was installed successfully on the Europipe jacket, known as Draupner E today [25]. The caisson penetrated into the seabed due to the weight of the structure an applied suction. The static system of the jacket ensures that the caisson is only loaded with vertical forces from the wave load. The caisson will not be pulled from the bottom because there is not enough time during a wave period.

Bucket foundations for offshore wind turbines will in the same way as a suction caisson be installed with the weight of the structure and applied suction. However, the weight of the structure is much lower so that more suction needs to be applied to penetrate the seabed. One major difference from a suction caisson is that a bucket foundation for offshore wind turbines will be subjected to large moments. This is due to the thrust force from the turbine. The stability of the foundation depends on the earth pressure on the skirt and the vertical bearing of the bucket.

3.2 Loads on the bucket foundation

For a monopile tower with a bucket foundation, all the environmental loads from wind, waves and current will be transferred to the foundation. Compared to traditional bottom fixed offshore structures, the bucket will be subjected to large vertical forces and even higher moments [10]. With the trend of turbines getting larger the foundation will have to support even larger vertical forces and moments. The stability of the foundation against overturning moment depends on the earth pressure on the skirt and the vertical bearing of the bucket. A tripod solution would resist overturning moment by combination of tension and compression on the upwind and downwind leg. The mono bucket solution would have to overcome the overturning moment by increasing the diameter and height of the skirt.

4 Stochastic and random process

Loads on an offshore wind turbine varies in time. Analysis in different software are usually done in the time domain. This means that the turbine is subjected to loads from wind, waves and current that varies in time. From a time domain analysis several parameters can be obtained. Maximum, minimum and mean are some of the parameters that can easily be distinguished from a time series. However, to make the data more accessible and easier to understand, one can transform the time series into the frequency domain. Vibration analysis is done in the frequency domain. The data is often transformed into a spectrum where several characteristics responses can be distinguished far more easily. Figure 4.1a shows an example of a measured time series and figure 4.1b shows the corresponding spectrum. For the support structure of an offshore wind turbine it is important that the natural frequency of the structure do not lie within the frequency range of external forces. This is to ensure that fatigue do not shorten the life time of the support structure.

(a) Measured time series   (b) Power spectrum of time series
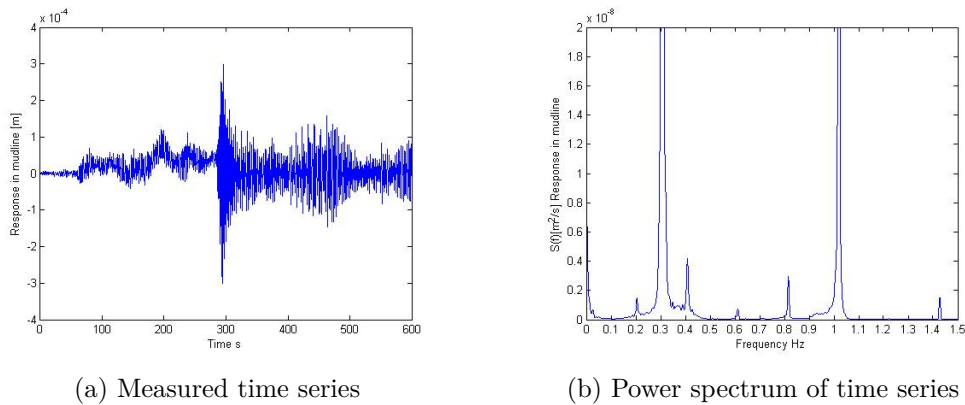
Figure 4.1: Example of a time series and the corresponding power spectral density spectrum

4.1 Description of random data

Random or stochastic events are time-varying events that cannot be reproduced or predicted in detail. For waves we simulate this by applying a random phase angle to each wave component and then sum up all wave components to produce a time series of the wave elevation. Analysis of random data is often done within a time interval where the statistical parameters of the process remain constant. This is referred to as a stationary process. A sea state is often considered stationary for 3 hours, while wind is considered stationary for 10 minutes [27].

To transform a time series to the frequency domain, Fourier transformation is used. The basic assumption of Fourier transformation is that random signals can be represented by

7

the sum of a number of wavelets [15]. Each wavelet have a specific amplitude, frequency and phase angle. The waves are represented as:

$$z_{wave}(t) = A_{wave} sin(f_{wave} * 2\pi * t + \phi_{wave}) \tag{4.1}$$

where

z_{wave}	elevation at time t	[m]
A_{wave}	wave amplitude	[m]
f_{wave}	wave frequency	[Hz]
ϕ_{wave}	wave phase angle	[rad]
t	time	[s]

An irregular wave made from a combination of 3 regular waves is shown in figure 4.2.
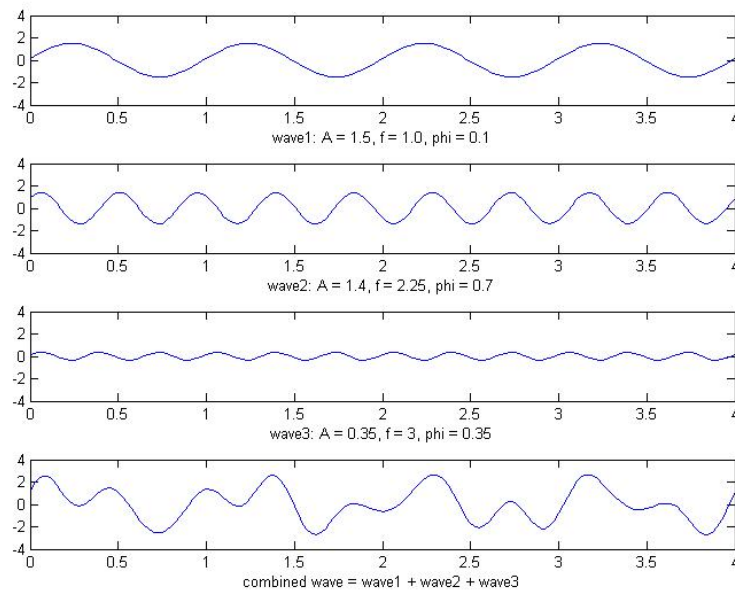
Figure 4.2: Three regular waves combined to an irregular wave

8

4.2 Time and frequency domain description

The Fourier transformation can be performed manually by representing the amplitude and phase angle as a function of frequency. However, there are developed several algorithms to perform the transformation in a standard manner for any given signal. One of the most commonly used algorithms is the Fast Fourier Transform or FFT. The FFT usually gives an output of the signal as a power spectral density spectrum rather than amplitude and phase angle as a function of frequency. The power spectral density per frequency is defined as: $\frac{1}{2}\frac{A_{wave}^2}{\Delta f}$ as a function of frequency.

In the same manner as a spectrum can be made from a time signal, a time signal can be made from a spectrum with the Inverse Fast Fourier Transformation, IFFT. Harmonic waves can be created based on the power spectral density at each separate frequency and a random phase. Since the phase is random it will not recreate the exact time series as the spectrum is made from, but the spectral parameters of the time series will be the same. IFFT is used when creating waves from a wave spectrum.

4.3 Main parameters and windowing of time series

To produce spectra based on time series of finite length, it is common to cut the time series into sections, M, of equal length. The spectral density of all sub-records are then averaged to a smoothed spectrum [5]. Each section have an equal number of data points, N, with a constant time step, Δt. By letting N be a power of 2, the computational time is very efficient. The frequency range of the power spectrum is only depends on Δt and is expressed by

$$f_N = \frac{1}{2\Delta t} \tag{4.2}$$

It is not always easy to have a sampling number in each section, M, that is a power of two. The sampling number depends on the length of the section and the time step. If the sampling number is below an integer of the power of two, some sharp peaks may be excluded and the spectrum is smoothed out [6]. If sharp peaks is of special interest, the sampling number in each section have to meet the criteria of being a power of two.

When the time series is cut into several sections, the block size of sampling is smaller than the original whole time series. Smaller block size makes the spectrum smoother, meaning that sharp peaks may not be captured. The discontinuity of the start and end of each finite length record causes leakage of spectral density [26] [5]. Loss of data can be prevented by using the technique of window. Each sub-record can have up to 50 % overlap. The resulting spectrum is an average of the original sections and the overlapping sections. Common used spectral windows are Hanning and Hamming which will not be presented here.

5 Waves

The main contribution to waves at open sea is the wind. A flat mirror-like surface can only occur in absolute absence of wind. A light breeze will create ripples in the water while higher wind velocities may cause waves that are several meters high. Stansell measured extreme waves in the north sea, about 100 miles east of the Shetland Islands, which gave freak waves of 24.19 meters during a 20 minute record [23]. A freak wave is frequently defines as when the crest-to-through wave height is more than twice the value of the significant wave height of the record.

5.1 Sea surface description

When observing the sea surface one will not experience several long crested waves travelling in the same direction. One will rather observe numerous waves travelling at what will seemingly be every direction. The crest length of each wave will also be of different length. The sea surface is best described as a random process. There has been developed several models to describe the random process of the sea surface.

The sea surface is best described by the wave elevation at a single point at sea over time. If one measures the elevation at a single point over time, the random sea in Figure 5.1 will result in a time series which is similar to that illustrated in Figure 5.2. The time varying signal can be transformed to a energy density spectrum as illustrated in Figure 5.3. The spectrum is commonly referred to as a wave spectrum. The time series and wave spectrum is meant as an illustration and is not an actual measurement of the random sea surface in Figure 5.1.

Figure 5.1: Actual sea surface
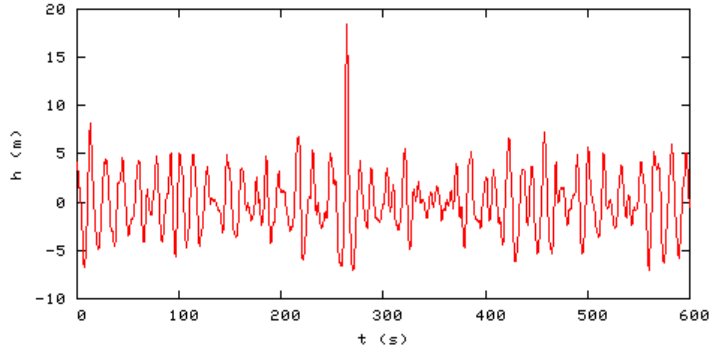
Figure 5.2: Single point time record of sea surface elevation
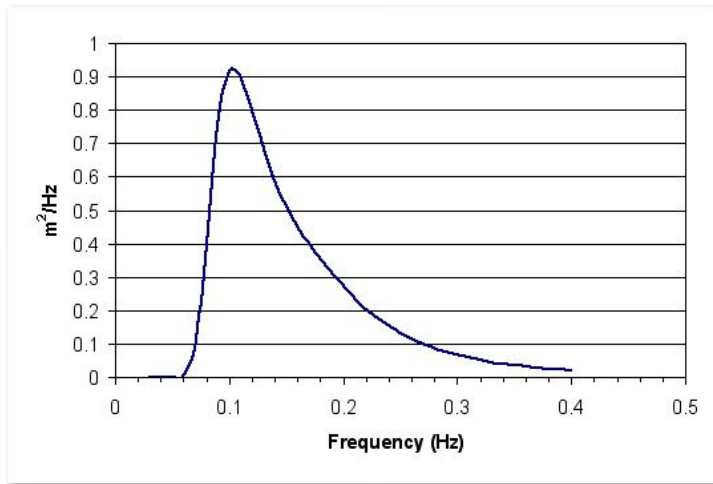
Figure 5.3: Wave spectrum of measured time record

5.2 Statistical description of waves

In practice, linear theory is used to simulate irregular sea and to obtain statistical estimates [7]. The wave elevation for a long crested wave can be written as a sum of of a large number of wave components.

$$\zeta = \sum_{j=1}^{N} \zeta_A sin(\omega_j t - k_j x + \epsilon_j) \tag{5.1}$$

Here ζ_A, ω_j, k_j and ϵ_j is the wave amplitude, circular frequency, wave number and random phase angle of wave component number j. The random phase angles ϵ_j are uniformly distributed between 0 and 2π and constant with time.The wave amplitude A_j can be expressed by a wave spectrum $S(\omega)$. The wave amplitude is expressed as

$$\frac{1}{2}A_j^2 = S(\omega_j)\Delta\omega \tag{5.2}$$

11

where $\Delta\omega$ is a constant difference between successive frequencies.

From the time series and wave spectrum as shown in figure 5.2 and 5.3, we can define some characteristic parameters. The significant wave height of the spectrum, H_S, is defined as the mean of the 1/3 highest waves in the time series. This is also equal to 4 times the standard deviation, σ, of the time series. From the wave spectrum we can find the standard deviation as the square root of the zeroth order moment of the spectrum, m_0. As for the time series, the significant wave height can be taken as 4 times the square root of m_0 from the wave spectrum. This usually gives a value close the significant wave height from the time series [7].

From the time series, one can find the mean zero crossing period T_z by dividing the measurement time by the number of zero up-crossings. This period can also be found from the wave spectrum as the square root of the zeroth moment over the second moment. The relationship between time domain and spectral parameters is given in table 1. The reader should be aware that the relationship below is valid for spectra based on frequencies in [Hz]. Frequency is chosen as Hz because wind and most of the thesis is described in Hz. Wave spectrum can also be defined with angular frequency [rad/s].

Table 1: Relation between Time Series and Spectral Parameters

Description	Relation
spectral moments (n = 0,1,2...)	$\int_0^\infty \omega^k S(\omega) d\omega$
variance or mean square	$\sigma^2 = m_0$
standard deviation or root-mean-square	$\sigma = \sqrt{m_0}$
significant wave height	$H_s \approx 4\sigma$
mean zero crossing period	$T_z = \sqrt{\frac{m_0}{m_2}}$
mean period of the spectrum	$T_m = \frac{m_0}{m_1}$
mean crest period	$T_c = \sqrt{\frac{m_2}{m_4}}$

The shape of the wave spectrum has been fitted with several curves. DNV suggest to use the Pierson-Moskowitz (PM) or JONSWAP spectrum which are frequently used spectrum [27]. The relationship between time domain representation of waves and the frequency domain representation of waves by a wave spectrum $S(f)$ is illustrated in figure 5.5.

The PM spectrum was originally proposed for fully developed sea with infinite fetch [19]. The shape was fitted to measurements taken during long periods of constant environmental conditions. The spectrum is based on the single parameter, average wind speed. The PM spectrum can be expressed by the significant wave height and peak period as

$$S_{PM}(f) = \frac{5}{16} \frac{H_s^2}{T_p^4 f^5} exp(-\frac{5}{4}(fT_p)^{-4}) \tag{5.3}$$

The relationship between T_z and T_p for the PM spectrum is given as

$$T_p = 1.41T_z \tag{5.4}$$

Here T_p is the peak of the spectrum, and must not be confused with the mean crest period T_z. Figure 5.4 shows a plot of the Pierson-Moskowitz spectrum for a given peak period and significant wave height.
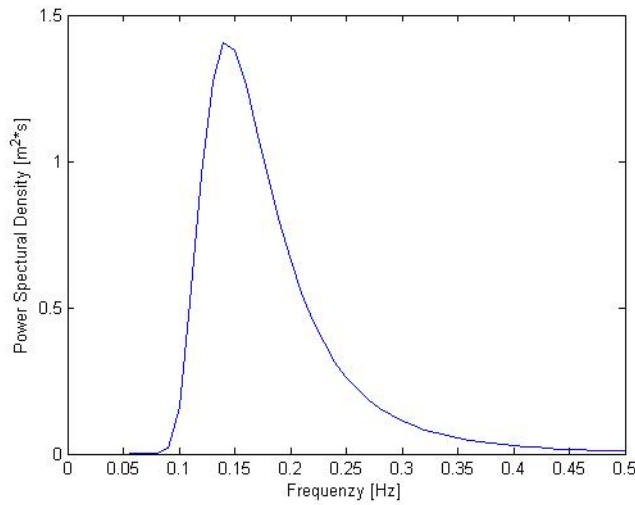
Figure 5.4: Pierson-Moskowitz spectrum for $H_s = 1.5$ m and $T_p = 7s$

The JONSWAP spectrum is an extension to the PM spectrum which includes limited fetch [9]. Further measurements of wave spectra was conducted during the Joint North Sea Wave Project. The JONSWAP spectrum represent sea states that are not fully developed under a certain wind condition. The result is a much steeper peak compared to the PM spectrum. As mentioned, the JONSWAP spectrum is an extension of the PM spectrum. The spectrum includes a non-dimensional peak shape parameter, γ. When the shape parameter is equal to 1, $\gamma = 1$, the JONSWAP spectrum is equal to the Pierson-Moslowitz spectrum. The spectrum also includes slope factors σ_a and σ_b which control the shape of the slope before and after T_p. According to DNV standards, typical average values for the parameters are $\gamma = 3.3$, $\sigma_a = 0.07$ and $\sigma_b = 0.09$ [27].

The peak enhancement factor will increase the total area under the spectrum. To ensure that the area under the JONSWAP represent the real energy density of the sea, the normalizing factor, α, is introduced. There are several representations of the normalizing factor. One representation is formulated below and can be found in [27].

$$S_{JS} = \frac{\alpha g^2}{(2\pi)^4} f^{-5} exp(-\frac{5}{4}(\frac{f}{f_p})^{-4})\gamma_{JS}^{exp(-0.5(\frac{f-f_p}{\sigma_{JS}*f_p})^2)} \tag{5.5}$$

Here g is the gravitational constant and

$$\sigma_{JS} = \begin{cases} \sigma_a = 0.07 & \text{for} \quad f \leq f_p \\ \sigma_b = 0.07 & \text{for} \quad f > f_p \end{cases} \tag{5.6}$$

$$\alpha = 5 * (H_s^2 f_p^4 / g^2) * (1 - 0.287 ln\gamma) * \pi^4 \tag{5.7}$$

The relationship between T_p and T_z for the JONSWAP spectrum differs from that of the PM spectrum. For $\gamma = 1$ one can use the relationship given by the PM spectrum in equation 5.4. For other values of, γ, one can use the relation

$$\frac{T_z}{T_p} = 0.6673 + 0.05037\gamma - 0.006230\gamma^2 + 0.0003341\gamma^3 \tag{5.8}$$
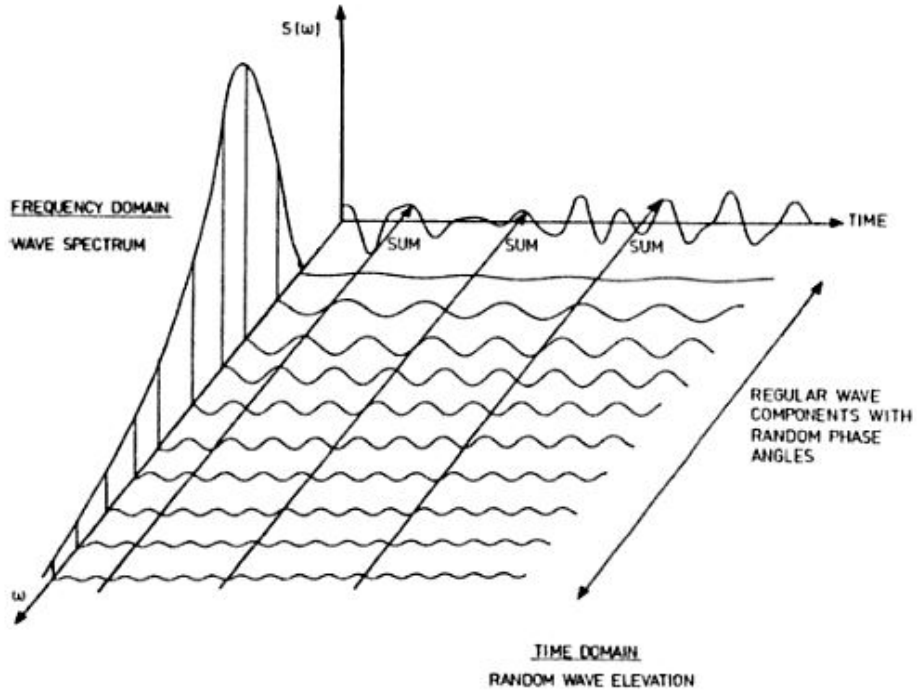
Figure 5.5: Connection between a frequency domain and time domain representation of waves in long-crested short term sea state [7]

6 Wind

6.1 Introduction

The wind velocity measured in a wind field shows variation in time, space and direction. Figure 6.1 shows a typical wind speed representation at a time instance. The figure shows that the mean wind speed increases with height. This variation is referred to as wind shear. The actual wind speed at any location varies in time and direction around its mean value. This is referred to as turbulence.
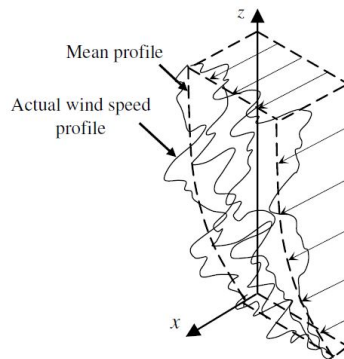
Figure 6.1: Actual wind speed profile [26]

6.2 Wind Shear

In the lower 2 kilometres of the earth's atmosphere, the wind speed is affected by friction with the earth's surface [16]. This effect is known as wind shear and reduces the wind speed from its undistributed value at 2 kilometres height to nearly zero at the surface. There are two main models commonly used to describe the wind shear effect: the logarithmic profile and the power law profile. Both profiles describes the mean wind as a function of height above the earth's surface. Both profiles are fitted curves to measured wind shear effects. The logarithmic profile and power law profile are described by equation 6.1 and 6.2 [16].

$$V_w(z) = V_{w,r} * \frac{ln\frac{z}{z_0}}{ln\frac{z_r}{z_0}} \tag{6.1}$$

$$V_w(z) = V_{w,r} * (\frac{z}{z_r})^{\alpha_{shear}} \tag{6.2}$$

with:

Table 2: Relation between Time Series and Spectral Parameters

Parameter	Description	Unit
$V_w(z)$	Mean wind speed at height z	[m/s]
$V_{w,r}$	Mean wind speed at reference height z_r	[m/s]
z_r	Reference height	[m]
z_0	Surface roughness length	[m]
α_{shear}	Power law coefficient	[-]

Values for the surface roughness length and power law coefficient can be found in standards. DNV suggest that the surface roughness length, z_0, for open seas with waves is between 0.001-0.01 and power law coefficient, α_{shear}, is 0.12 [27]. Values for other wind climates is listed in the standards.

A comparison of the log and power law profile is shown in Figure 6.2a for a mean wind of 10 m/s at a reference height of 10 meters. The figure clearly shows the difference of wind speed for a hub height of 90 to 100 meters. In early stages of the design process it is important to choose which model to use, as this will influence the load calculations and power production. Design programs for turbine load often requires the mean wind at hub height. Figure 6.2b shows the wind profiles for a mean wind of 12 m/s at 60 meters height. The two models will be closer at the hub height. The difference will nearly cancel over the rotor disk.
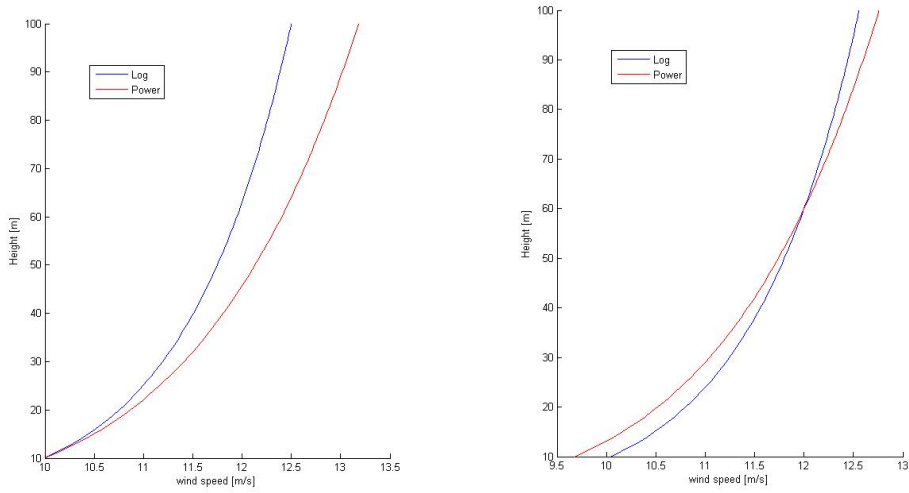
(a) Mean wind speed 10 m/s at height 10 m

(b) Mean wind speed 12 m/s at height 60 m

Figure 6.2: Mean wind speed according to log and power law model

6.3 Wind turbulence

In addition to the mean wind found from wind shear there will be a time varying fluctuation in the wind speed. The turbulent fluctuation in the wind is superimposed on the steady state mean wind to find the wind speed at each time step. Figure 6.3 shows a realization of wind data sampled at 8 Hz [16]. The data has a mean of 10.4 m/s and a standard deviation of 1.63 m/s. The data clearly shows that variation is irregular and that turbulence can not be described deterministic. Turbulence is best described statistically.
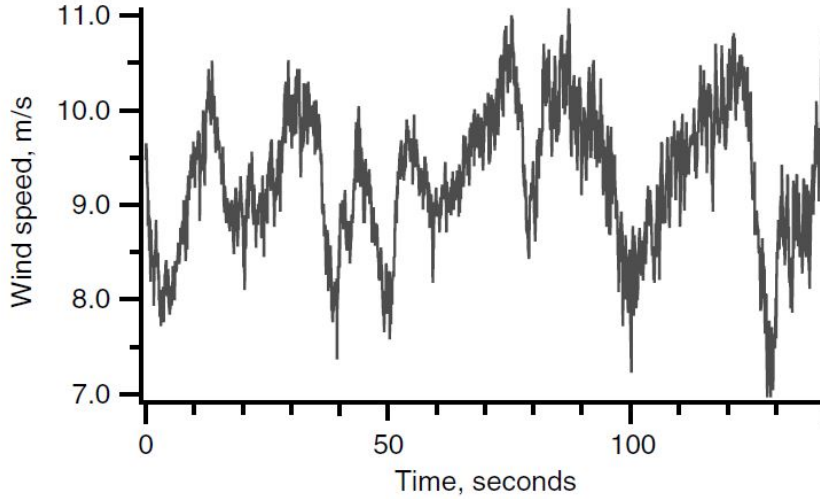
Figure 6.3: Typical plot of wind speed vs. time for a short period [16]

The statistics of turbulence is described by Freris [8].Turbulence is the deviation of the instantaneous wind speed $U(t)$ from the steady mean shear wind speed $\overline{U}$

$$u(t) = U(t) - \overline{U} \tag{6.3}$$

The variability of the wind speed is described in terms of the variance, σ_u^2, given as

$$\sigma_u^2 = \frac{1}{T} \int_{t_0 - \frac{T}{2}}^{t_0 + \frac{T}{2}} [U(t) - \overline{U}]^2 dt \tag{6.4}$$

Where T is the time of the whole series. The turbulence intensity is defined as the standard deviation of the time varying wind speed divided by the mean wind speed, in percentage

$$I_t = \frac{\sigma}{\overline{U}} [\%] \tag{6.5}$$

The intensity is dependent on height and roughness of the terrain. Rougher terrain and lower altitude gives higher turbulence intensity. Design standards suggests given turbulence intensities based on roughness and altitude at different sites.

17

Manwell et al gives a good description of the fluctuations in the wind [16]. The fluctuations in the wind can be thought of as resulting from a composite of sinusoidally varying wind superimposed on the mean steady wind. These sinusoidal variations will have a variety of frequencies, amplitude and phases.

Spectrum are often used to describe functions of frequency. The function that characterise turbulence as a function of frequency is known as 'power spectral density' function. Since the average value of a a sinusoidal function is zero, the amplitude are characterized in terms of their mean square values. The average power in the turbulence over a range of frequencies may be found by integrating the power spectral density function between the two frequencies. The integral over all frequencies is equal to the total variance. An often used power spectral density function is the von Karman power spectral density function given by:

$$S(f) = \frac{\sigma_u^2 4(L/U)}{[1 + 70.8(fL/U)^2]^{5/6}} \tag{6.6}$$

where f is the frequency (Hz), L is the integral length scale, and U is the mean wind speed at the height of interest. The integral scale length, L, is given in standards. Other power spectral density functions are used in wind engineering applications. Turbulence spectra over sea generally contain even greater low frequency content [26]. DNV recommends the Kaimal spectrum which is given by:

$$S(f) = \frac{\sigma_u^2 4(L/U)}{[1 + 6(fL/U)]^{5/3}} \tag{6.7}$$

Figure 6.4a shows a von Karman power spectral density function with logarithmic scale. It also shows sample data for comparison. Figure 6.4b shows the spectrum for the same mean wind and standard deviation without logarithmic scale. Most of the energy is in the lower frequencies.
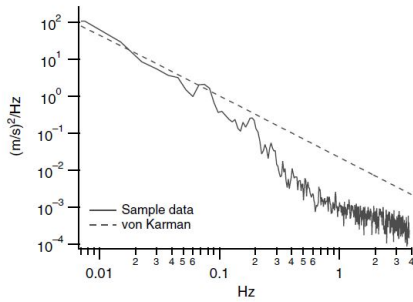
(a) Von Karman Spectrum in logarithmic scale [16]
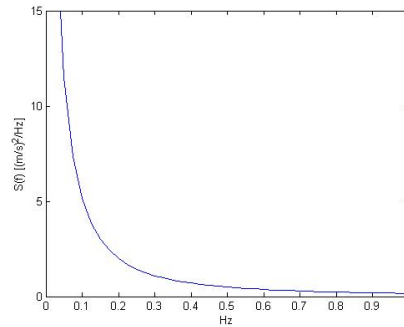
(b) Von Karman spectrum

Figure 6.4: Wind spectrum for mean wind 10.4 m/s and standard deviation 1.63 m/s

6.4 Rotational Spectrum

The wind spectrum shown above is for a stationary observer. This means that if you where to measure the wind, the measuring device would stand still. The blades on a wind turbine is rotating. What would happen if the wind velocity measuring device was attached to the blades? Compared to a stationary spectrum a rotational spectrum will have several peaks in the power spectrum.

If one consider a gust of velocity $u(t)$ that have a lateral and vertical dimension that is smaller than the radius of the blade. Every time the blade sweeps through the gust, the wind velocity experienced by the blade will increase from the mean wind velocity U to $U + u$. A stationary observer will only experience the mean velocity U or $U + u$. This effect is illustrated in Figure 6.5.
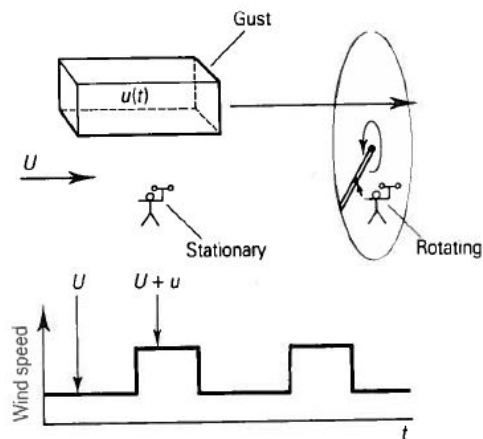
Figure 6.5: Rotational sampling [8]

The rotational sampled spectrum is derived from the autocorrelation function at a point on the rotating blade. The derivation of the rotational sampling assumes Taylor's frozen turbulence hypothesis which means that the instantaneous wind speed at a point C at time τ is the same as point B a distance $\overline{U}\tau$ upwind of C at time t = 0 [4]. This is illustrated in Figure 6.6. Further, the autocorrelation function following the blade at point r on the blade is the same as the cross-correlation function between the along wind fluctuations at point A and B given as:

$$\kappa_u^0(r, \tau) = \kappa_u^0(\overrightarrow{s}, 0) \tag{6.8}$$

Where $\kappa_u^0(r, \tau)$ is the autocorrelation and $\kappa_u^0(\overrightarrow{s}, 0)$ is the cross-correlation. The radius of the blade is r and τ is the time. $\overrightarrow{s}$ is the vector between A and B. The power spectrum for rotational sampling can be found by taking the Fourier transform of $\kappa_u^0(\overrightarrow{s}, 0)$. Fully mathematical derivation of the rotational sampling power spectrum can be found in Burton and Freris [4] [8].

19
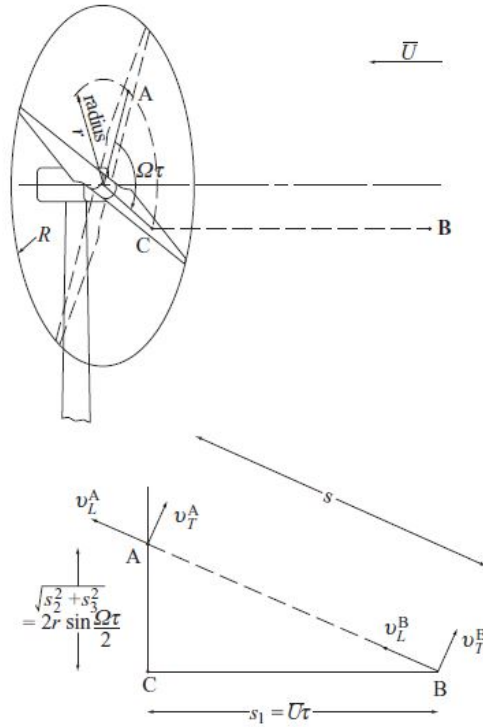
Figure 6.6: Rotational sampling [8]

The rotational sampling was investigated by D.Tcherniak et al. for operational modal analysis considerations [24]. Some conclusions about the rotational sampling spectrum can be made. The spectrum have peaks at the rotational frequency and its harmonics. Meaning that the spectrum will have peaks at all nP frequencies, where n = 1,2,3.... The peaks are more severe for increasing radius. The peaks are not sharp, but have rather thick tails. These observations are supported by Freris and Burton [8] [4]. Figure 6.7 shows an analytical solution for the rotational power spectrum for mean wind speed of 8 m/s. Figure 6.8 shows a numerical simulated spectrum for mean wind of 18 m/s.
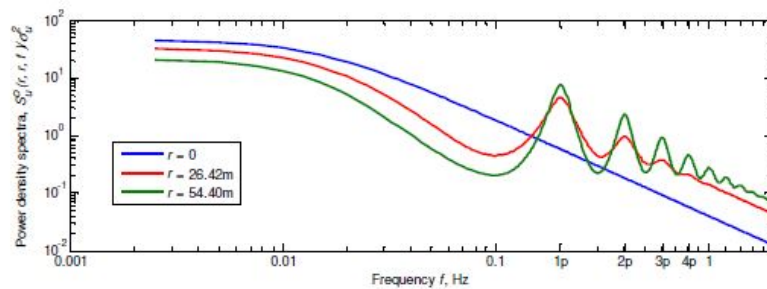
Figure 6.7: Analytical rotational spectrum for mean wind of 8 m/s [24]
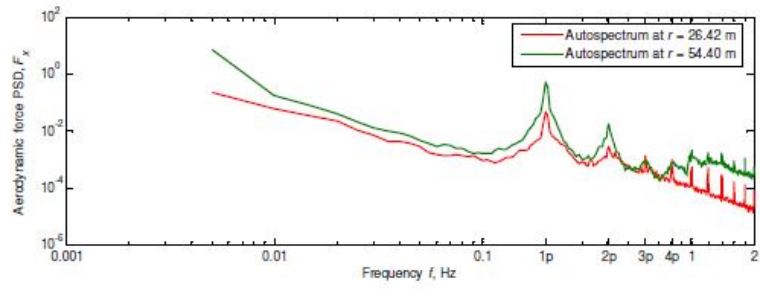
Figure 6.8: Numerical rotational spectrum for mean wind of 18 m/s [24]

7 Dynamics of wind turbines

7.1 Basics of dynamics

Basic dynamics is best illustrated by a single degree of freedom mass-spring-damper system as shown in Figure 7.1. An offshore wind turbine system can be regarded as being constructed of a number of coupled multi degree of freedom mass-spring-damper systems [18].
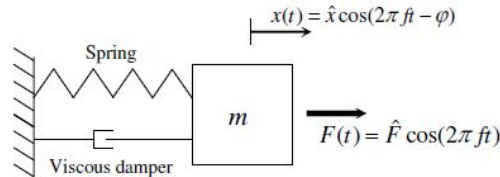
Figure 7.1: Single degree of freedom mass-spring-damper system

When the mass is exposed to a harmonic excitation, $F(t)$, the magnitude and phase of the resulting displacement, x, strongly depends on the frequency of the excitation. There are three steady state response regions that can be distinguished as shown in Figure 7.2.

a. Quasi-static

b. Resonance

c. Inertia dominated
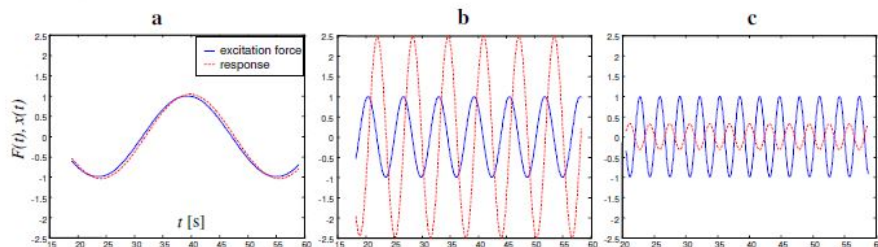
Figure 7.2: a) Quasi-static b) resonant and c) inertia dominated response. The blue line represents excitation and red line displacement [26]

For the quasi static response, the displacement of the mass nearly follows the time varying force. For the resonant response, the inertia force and spring force almost cancel out which results in a response that is much larger than it would be statically. The resulting amplitude depends on the damping in the system. For the inertia dominated response, the mass is not able to follow the the excitation. The response is low an almost in counter phase with the excitation.

7.1.1 Single degree of freedom system

Figure 7.1 represent a single degree of system. The mass, m, is fixed to a wall with a spring stiffness, k, and a linear viscous damper with damping coefficient, c. For a single degree of system we have the following equation of motion:

$$m\ddot{u}(t) + c\dot{u}(t) + ku(t) = F(t) \tag{7.1}$$

For an un-damped system we will have free oscillation. This means that the vibration takes place without external influence. In real life there will always be some sort of damping that will stop the oscillation if there are no external forces acting on the system. For a single degree of freedom system without damping the equation of motion can be written as

$$m\ddot{u}(t) + ku(t) = F(t) \tag{7.2}$$

which has a natural frequency of:

$$\omega_0 = \sqrt{\frac{k}{m}} \tag{7.3}$$

The natural frequency is only dependent on the mass and stiffness of the system.

7.1.2 Multi degree of freedom system

A single degree of system will only describe one frequency, namely the natural frequency. In structural dynamics the structure will have several eigen-frequencies which can coincide with external excitations. For an offshore wind turbine the most obvious external excitations are the 1P and 3P frequencies of the blades passing the tower and the frequency of the wave loads. A multi degree of system can be solved by modal analysis and the eigenvalue problem. The equation of motion is now described on matrix format

$$\mathbf{M\ddot{r}} + \mathbf{C\dot{r}} + \mathbf{Kr} = \mathbf{Q}(t) \tag{7.4}$$

where $\mathbf{M}$, $\mathbf{C}$ and $\mathbf{K}$ is the mass, damping and stiffness matrix of the structure. $\mathbf{Q}(t)$ is the load vector and $\mathbf{r}$ is the nodal displacement vector. For an undamped system with free vibration the system can be expressed as

$$\mathbf{M\ddot{r}} + \mathbf{Kr} = \mathbf{Q}(t) \tag{7.5}$$

In modal analysis it will be more rational to express the displacements in terms of mode shapes Φ. The mode shapes can be found by solving the eigenvalue problem expressed as

$$[\mathbf{K} - \omega^2 \mathbf{M}]\Phi = 0 \tag{7.6}$$

The non-trivial solution for the eigenfrequencies can be found when

$$\omega^2 = det|\mathbf{K} - \omega^2\mathbf{M}| = 0 \qquad (7.7)$$

There are several numerical methods for solving the eigenvalue problem for large systems. They will however not be described here. Solving the system will give the same number of eigenfrequencies as there are number of degrees-of-freedom in the system.

7.2 Soft or stiff wind turbine systems

An offshore wind turbine is subjected to time varying loads from wind, waves and current. The loads will occur with different frequencies. The support structure for the turbine will have to be designed for several excitation frequencies. The most obvious source of excitation in a wind turbine systems comes from the rotor. The 1P and 3P frequencies from the rotor blades passing the tower will create excitations. To avoid resonance in the structure the first natural frequency of the structure should be designed such that it does not coincide with either 1P or 3P excitations. There are three possible intervals in which the first natural frequency can lie in to avoid the 1P and 3P frequency [26]. A very soft structure with the first natural frequency below 1P, called a soft-soft structure. A soft-stiff structure with the first natural frequency between 1P and 3P, or a stiff-stiff structure with first natural frequency above 3P. Figure 7.3 represent the excitation frequencies from the blades and the three different intervals for the support structure. The horizontal axis is frequency and the vertical axis represent an arbitrary response without value.
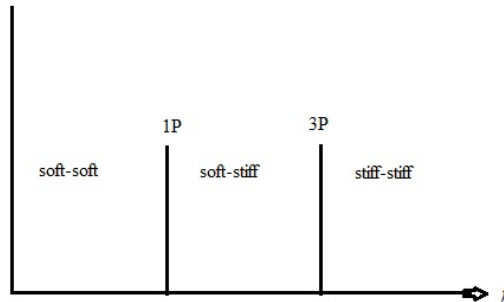
Figure 7.3: Soft to stiff frequency interval for a three bladed, constant rotational speed wind turbine

7.3 Support structure

7.3.1 First natural frequency

The support structure of a wind turbine can be modelled as a cantilever beam with a top mass, m_{topp}, as shown in Figure 7.4. This will represent a mass-spring-damper system. The mass is given by the density of material and the spring stiffness by the bending

flexibility of the beam. Even though this is an idealized model it will represent the basic dynamics of a wind turbine system.
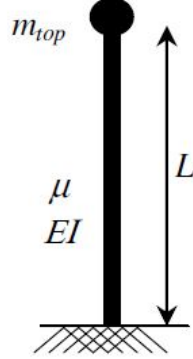
Figure 7.4: Structural model of a flexible wind turbine system [26]

For this model consisting of a uniform beam with a top mass and a fixed base, it can be shown that the following approximation for the first natural frequency is valid [26].

$$f_{nat}^2 \cong \frac{3.04}{4\pi^2} \frac{EI}{(m_{top} + 0.227\mu L)L^3} \tag{7.8}$$

with the parameters

Parameter	Description	Unit
f_{nat}	first natural frequency	[Hz]
m_{top}	top mass	[kg]
μ	tower mass per meters	[kg/m]
L	tower height	[m]
EI	tower bending stiffness	[Nm^2]

For a thin walled structure the second moment of inertia can be expressed as:

$$I \cong \frac{1}{8}\pi D_{av}^3 t_w \tag{7.9}$$

The tower mass per meter as:

$$\mu = \rho_{steel}\pi D_a v t_w \tag{7.10}$$

If we introduce the parameter, a

$$a = \frac{m_{top}}{\rho_{steel}\pi D_{av}t_w L} \tag{7.11}$$

equation 7.8 can be re-written to:

$$f_{nat} \cong \frac{D_{av}}{L^2} \sqrt{\frac{E}{104(a + 0.0227)\rho_{steel}}} \qquad (7.12)$$

where:

Parameter	Description	Unit
t_w	tower wall thickness	[m]
D_{av}	tower average diameter $= D - t_w$	[m]
ρ_{steel}	density of steel	[kg/m^3]

Equation 7.12 is applied to the "NREL offshore 5-MW baseline wind turbine", which is an offshore reference wind turbine described by Jonkmann et al. [14]. This is a three-bladed variable speed wind turbine with a rated rotor speed of 12.1 rpm. For simplicity only the rated rotor speed will be considered. The rated speed will give a 1P frequency of 0.2 Hz and a 3P frequency of 0.6 Hz. Main parameters for the turbine is listed in table 3. The density of steel is 7850 kg/m^3, the effective density of steel includes additional weight for paint, bolts, welds and flanges which are not accounted for in the tower thickness data.

Table 3: Main parameters for the NREL offshore 5-MW baseline wind turbine

Hub Height	90 m
Rated Rotor Speed	12.1 rpm
Rotor Mass	110 000 kg
Nacelle Mass	240 000 kg
Effective density of steel	8 500 kg/m^3

From the data given in table 3 we can calculate diameters of the tower for given natural frequencies. In this calculations the conical shape of the tower will be disregarded and the diameter will be taken as an average over the whole support structure. The thickness is set to an average of 23 mm. A soft-soft structure will for the given 1P and 3P frequencies have for example a natural frequency of 0.15 Hz, soft-stiff 0.4 Hz and stiff-stiff 0.7 Hz. The results from applying Equation 7.12 are given in Table 4.

Table 4: Required diameters for different natural frequencies

Type	f_{nat}	Diameter
Soft-soft	0.15 Hz	3.6 m
Soft-stiff	0.4 Hz	7.1 m
Stiff-stiff	0.7 Hz	10.6 m

The results clearly show the different requirements of diameter for different first natural frequencies. From an investment point of view, it will be best to choose the softest support structure as this has the smallest diameter. However, these calculations are

only to demonstrate how the support structure influence the natural frequency of the structure. There are many other influences on a real offshore wind turbine support structure. There are other excitation frequencies than the 1P and 3P frequencies generated from the blades. Also, the support structure itself will have more than the first natural frequency which needs to be considered.

7.3.2 Second natural frequency

By solving the eigenvalue problem for the wind turbine system, it is possible to find several mode shapes and the belonging natural frequency for this mode shape. The flag pole described in figure 7.4 is now modelled on matrix form. The support structure is divided into beam elements with its belonging mass and stiffness matrix. The mass and stiffness matrix for each element is added in a global mass and stiffness matrix which are solved by the eigenvalue problem described in section 7.1.2. The resulting eigen-frequencies for the diameters calculated above i presented in Table 5.

Table 5: Required diameters for different natural frequencies

Type	first eigenfrequency	second eigenfrequency	Diameter
Soft-soft	0.15 Hz	1.9 Hz	3.6 m
Soft-stiff	0.4 Hz	3.8 Hz	7.1 m
Stiff-stiff	0.7 Hz	6.1 Hz	10.6 m

For all the diameters the second eigen-frequency is well above the 3P frequency. The calculations are meant as an illustration. For a real turbine, the frequencies will be considerably lower. Especially the second eigen-frequency. This is because the support structure is not clamped in the base, but will have a stiffness from the soil.

7.4 Dynamic response

The structure is subjected to dynamic response from external forces and the rotation of the blades. Monitoring of the response in the bucket foundation under operational mode was performed by Ibsen et al. [12]. The monitoring was performed without the influence of waves. The structure is subjected to the rotational frequency of the rotor referred to as 1P which will cause responses in the foundation. The structure is also subjected to responses at the blade passing frequency which is referred to as 3P. The foundation will have responses at the first natural frequency as this is close to the rotational frequency of the rotor. The blades have several modes within the frequency range. There is still a need to understand the eigen-modes of the blades and how they will effect the response in the structure.

The fatigue on the foundation was investigated by VAN DER TEMPEL [26]. In his research he found responses at the 3P, 6P and 9P for the tower top which comes from the blade passing frequency. In the foundation there were response at the first natural frequency, a small response around the 3P frequency and small response around the second natural frequency of the structure.

7.5 Considerations for larger turbines

7.5.1 Structural properties

Increasing the rotor diameter will have a direct influence on the dynamic behaviour of the structure. As shown in Figure 2.1, Section 2.2, the weight of the blade will increase with an exponent of 2.6 with increasing length. This means that the top mass will increase considerably. Most likely, the weight of the nacelle will also increase which will further increase the top mass. From equation 7.8, we can see that the natural frequency of the structure will decrease if the top mass increases.

A natural consequence of increasing the rotor diameter is that the length of the tower have to be increased to have sufficient clearance to the waterline. From Equation 7.8 we can see that increasing the length of the support structure will decrease the natural frequency of the structure. The influence on structural properties for larger rotors can be calculated approximately by a simple scaling of structural properties. One way of scaling is to introduce a scaling factor that takes the ratio between the original rotor diameter and the increased diameter [3] [17]. The scaling of structural parameters can be defined as:

$$SF = \frac{R_{tip}}{R_{tip,REF}} \tag{7.13}$$

This scaling factor takes the radius of the wanted larger blade divided by the radius of the reference blade. Dimensions is assumed to scale linearly, while other parameters like mass and the moment of inertia will scale by a higher order depending on the dimensions involved. The mass of the structure will typically scale cubically. If the density of the material is the same, the volume consists of a cross sectional area times the length. For a circular cylindrical tower without conical shape we have for the mass

$$M \propto \rho \frac{\pi}{4}(D_{outer}^2 - D_{inner}^2)L \propto SF^3 \tag{7.14}$$

where, ρ, is the density of the material, D, is the diameter and, L, is the length of the cylinder. The moment of inertia, I, is defined as:

$$I \propto \frac{\pi}{64}(D_{outer}^4 - D_{inner}^4) \propto SF^4 \tag{7.15}$$

The moment of inertia scales with the power of four. For a uniform bar with elasticity, E, and moment of inertia, I, that is clamped on one side, the natural frequency are proportional to:

$$f \propto \frac{1}{2\pi}\sqrt{\frac{EI}{ML^3}} \propto SF^{-1} \tag{7.16}$$

With a uniform scaling factor, constant density for the material and a constant elasticity, this will imply that the natural frequency decreases with SF^{-1}, with increasing blade size. For a soft-stiff structure, this means that with increasing blade diameter the natural frequency of the structure will get closer to the 1P frequency.

7.5.2 Rotational speed

There are several parameters that influence the power capture of the turbine. If one takes a blade optimized for aerodynamic power, it is captured through its airfoils and twist along the blade to make the angle of attack optimal per airfoil. The power will depend on the relation between the rotor speed and wind speed [16]. We say that the turbine has an optimal tip speed ratio. This is the ratio between the speed of the blade tip and the wind speed and is defined as:

$$\lambda = \frac{V_{tip}}{\overline{V}} = \frac{\Omega R}{\overline{V}} \tag{7.17}$$

where λ is the tip speed ratio, V_{tip} is the speed of the blade tip and $\overline{V}$ is the mean wind speed. From the definition of the turbine [14], we find that the optimal tip speed ratio of the turbine is 7.55. From Equation 7.17, we can define the tip speed ratio by the 1P frequency and the diameter of blade

$$\lambda = \frac{V_{tip}}{\overline{V}} = \frac{\Omega R}{\overline{V}} = \frac{f_{1p}\pi D_{rotor}}{\overline{V}} \tag{7.18}$$

By rearranging the above equation we can find how the 1P frequency change with increasing rotor diameter

$$f_{1p} = \frac{\lambda \overline{V}}{\pi D_{rotor}} \tag{7.19}$$

This means that for a fixed optimal tip speed ratio the rotational frequency of the rotor will decrease when the diameter increase. If we consider the NREL reference turbine with optimal tip speed ratio of $\lambda = 7.55$ and use the rated wind speed of $\overline{V} = 11.4m/s$, we can see how the rotational frequency will change with increasing blade length.
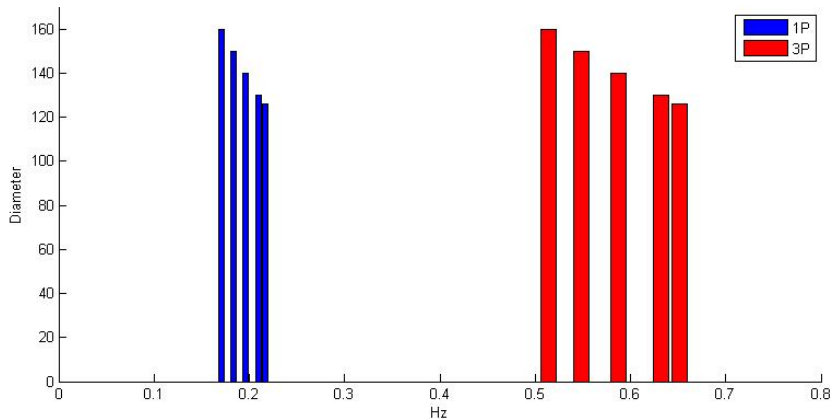

Figure 7.5: Changes in rotational frequency with increasing rotor diameter

8 Natural frequency considerations for support structure

8.1 The turbine in turbulent flow

An operational turbine will have rotors that rotates through a three-dimensional turbulence field. The turbulence field may be described by the correlated turbulence effects. A representation of a turbulence field is shown in Figure 8.1. This field covers an area of 100 by 100 meters at wind speed of 10 m/s with a turbulence intensity of 12% [26]. The figure clearly shows areas of higher and lower wind speeds than the mean wind speed.
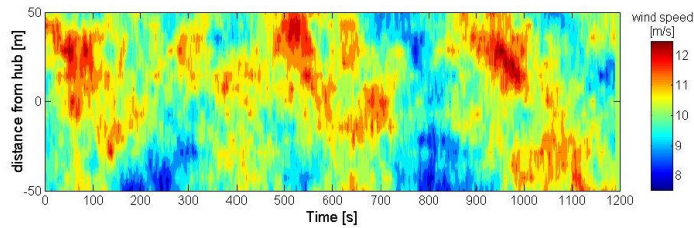
Figure 8.1: Turbulent eddies in a wind field [26]

When a rotating blade passes through a turbulent eddy, the strip that passes through will experience a short period of higher or lower wind speeds. Figure 8.2 shows a blade passing trough an eddy taken from the time interval from 500 to 550 seconds from the turbulent field in the figure above. The blade will pass through the eddy several times and experience a load peak each time it passes. This will be a load peak at the rotational frequency referred to as 1P. For a three bladed wind turbine there will also be a load peak at the 3P frequency. This is shown in the lower illustration in Figure 8.2.
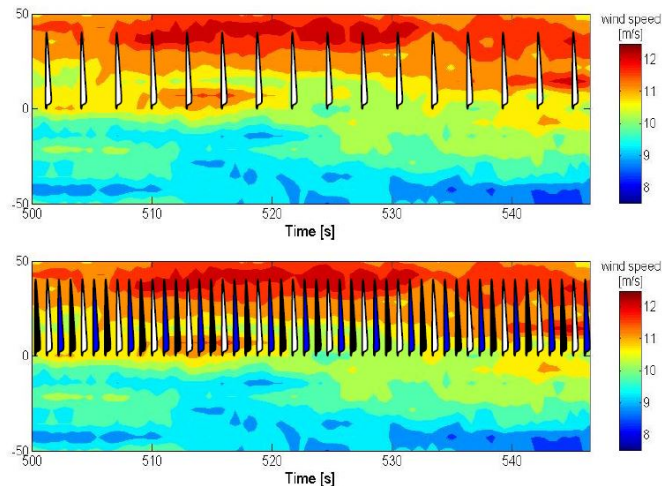
Figure 8.2: Single blade passing through turbulent eddy (above) at 1P frequency. All three blades (below) passing through the eddy at 3P frequency [26]

As described in Section 7.2 there are three solutions for the support structure when considering the rotational frequency of the turbine blades. However, since the mean wind will change over time, the 1P and 3P frequency will become a frequency band for a variable speed turbine. This means that the natural frequency of the soft structure will have to be below the lowest frequency in the 1P frequency band. The natural frequency of the soft-stiff structure will have to be between the 1P and 3P frequency band while the stiff structure will have to be above the highest frequency in the 3P band.
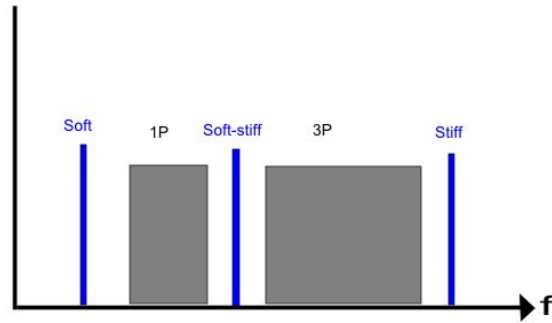
Figure 8.3: Rotational frequency band for a variable speed wind turbine

8.2 Turbulent blade load

When we transform the wind spectrum observed by a stationary observer to that observed by rotational observer the power spectrum for wind turbine blade forces will have peaks at the rotational frequency and its multiples. This means that we have a peak in the power spectrum at 1P, 2P, 3P etc. The second natural frequency of the support structure is much higher than that of the first natural frequency and is most likely well clear of the 3P frequency domain. However, it may coincide with the higher order rotational frequencies of the rotational sampling.
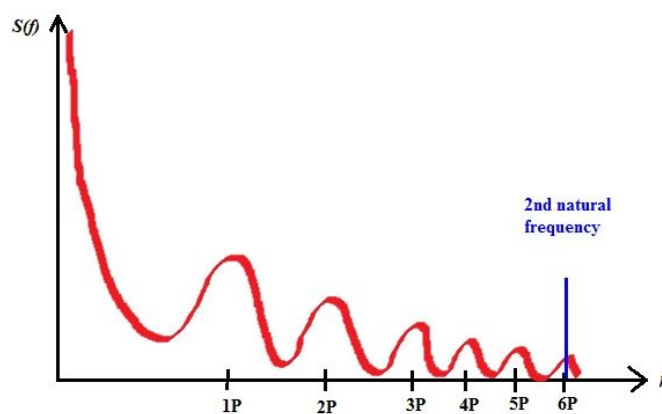
Figure 8.4: Rotational sampling of turbine blade forces

8.3 Wave excitation

Waves will be a source of excitation for offshore wind turbines. Wave frequencies are generally lower than the rotational frequency of the turbine. Still, waves come in various periods and will span in a wide range in the frequency band. Figure 8.5 shows an example of the Pierson Moskowitz spectrum for significant wave height of 2 meters and a peak period of 7 seconds. We can see that the natural period of a structure with natural frequency of 0.3 Hz is within the frequency band of the power spectrum. Naturally, the waves will give excitation to the structure. It is still important that the natural frequency of the structure is not to close to the peak period of waves that will occur often to avoid resonant behaviour.
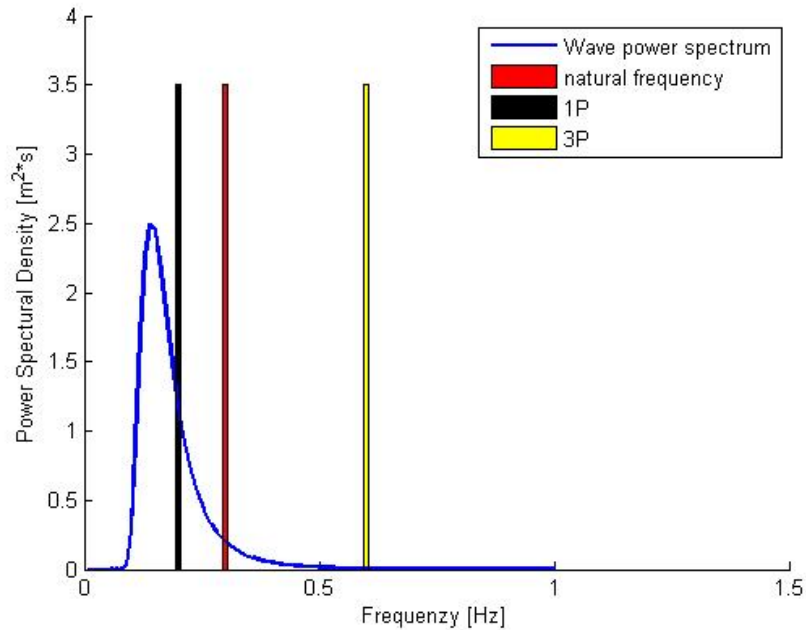
Figure 8.5: Natural frequency versus wave spectrum for $H_s = 2$m and $T_p = 7$s

Figure 8.6 shows the Pierson Moskowitz spectrum for the same significant wave height of 2 meters, but a peak period of 4 seconds. The peak of the spectrum is now very close to the natural frequency of the structure. This may cause resonant behaviour, which will reduce the lifetime of the support structure due to fatigue damage.
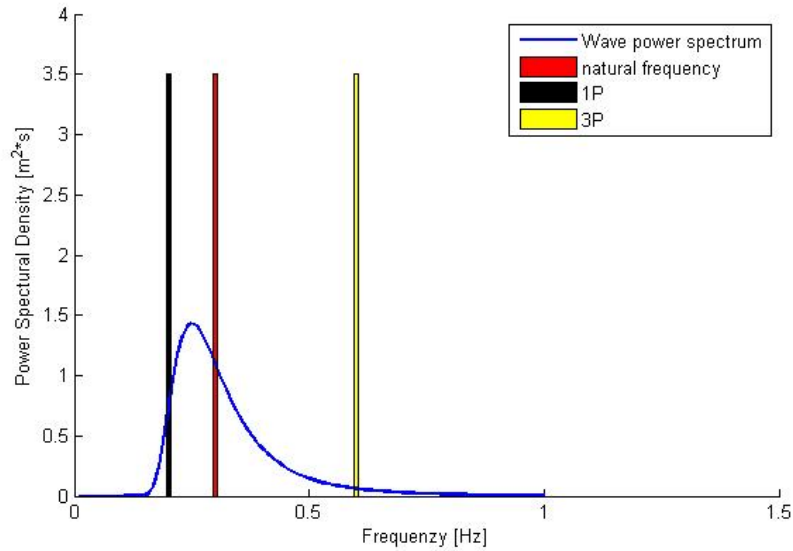
Figure 8.6: Natural frequency versus wave spectrum for $H_s = 2$m and $T_p = 4$s

8.4 Aerodynamic damping

Resonant behaviour is reduced as the wind loading on the rotor adds damping to the system. The tower top displacement and the total fatigue damage is reduced because of damping. The effects of aerodynamic damping is described by VAN DER TEMPLE [22]. "When the tower top is moving forward, the blades experience a small increase of wind speed and will respond to it aerodynamically. The response is such that an extra aerodynamic force will counteract the tower top motion, so the eventual excursion of the tower top due to the induced tower top velocity will be less. When the tower top moves backward the aerodynamic force decreases, again reducing the tower top motions". When this effects is included in the equation of motion it will act as damping.

9 Model Description

The model is a 5 MW reference turbine commonly known as the "NREL offshore 5-MW baseline wind turbine" [14]. The turbine is supported by a mono tower, a transition piece and a bucket foundation in the seabed. There is a FEM model of the soil to provide realistic soil conditions. The supporting structure and FEM soil model is provided by Statkraft and the author has not had any design decisions in the support structure and soil model. The model is designed for a water depth of 45 meters. A general 3D perspective of the model is shown in figure 9.1.

Figure 9.1: 3D perspective of the offshore wind turbine for 45 meters water depth

9.1 Turbine

The turbine is a conventional three-bladed upwind variable-speed variable blade-pitch-to-feather-controlled turbine. This is a reference turbine developed mainly for concept studies and research programs. It is defined by Jonkm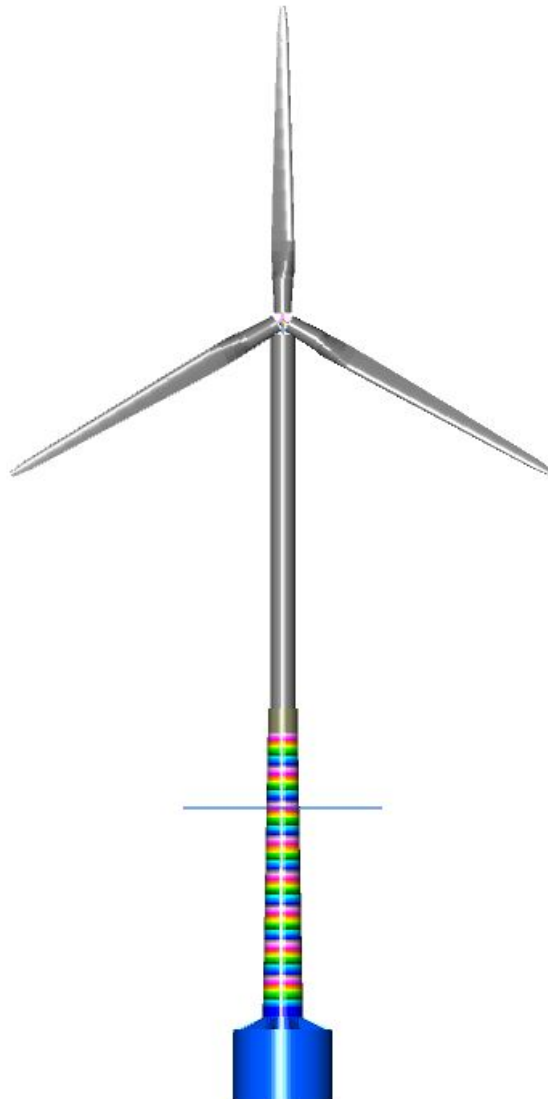an et al. [14]. The design is based on broad design information from published documents of turbine manufactures. However, since detailed data is unavailable, conceptual model studies was used to define the turbine. Main parameters for the turbine is presented in the table 6 below.

Table 6: Main properties for the NREL-5-MW Baseline Wind Turbine

Rating	5 MW
Rotor Orientation, Configuration	Upwind, 3 Blades
Control	Variable Speed, Collective Pitch
Rotor Hub Diameter	126 m, 3 m
Hub Height	98 m
Cut-in, Rated, Cut-Out Wind Speed	3 m/s, 11.4 m/s, 25 m/s
Cut-in, Rated Rotor Speed	6.9 rpm, 12.1 rpm
Rotor Mass	110 000 kg
Nacelle Mass	240 000 kg

From the cut-in rotor speed to the rated rotor speed we can see that the 1P frequency domain of the rotor is 0.115 Hz to 0.2 Hz. The 3P frequency domain will hence be 0.345 Hz to 0.6 Hz.

The blades are pitched controlled, meaning that they will rotate to reduce the force from the wind when the wind velocity increases over rated. The pitching angle against wind speed is listed in table 7.

Table 7: Wind speed versus pitch angle

Wind speed [m/s]	Pitch angle [°]
11.4 -rated	0
12	3.83
13	6.60
14	8.70
15	10.45
16	12.06
17	13.54
18	14.92

The thrust and torque curves for the rotor is shown in figure 9.2. We can see that maximum thrust appears at rated speed. When the wind speed goes above rated, the blades are pitched and there is a decrease in the thrust. The torque reaches its maximum at rated and is constant for increasing wind speeds.
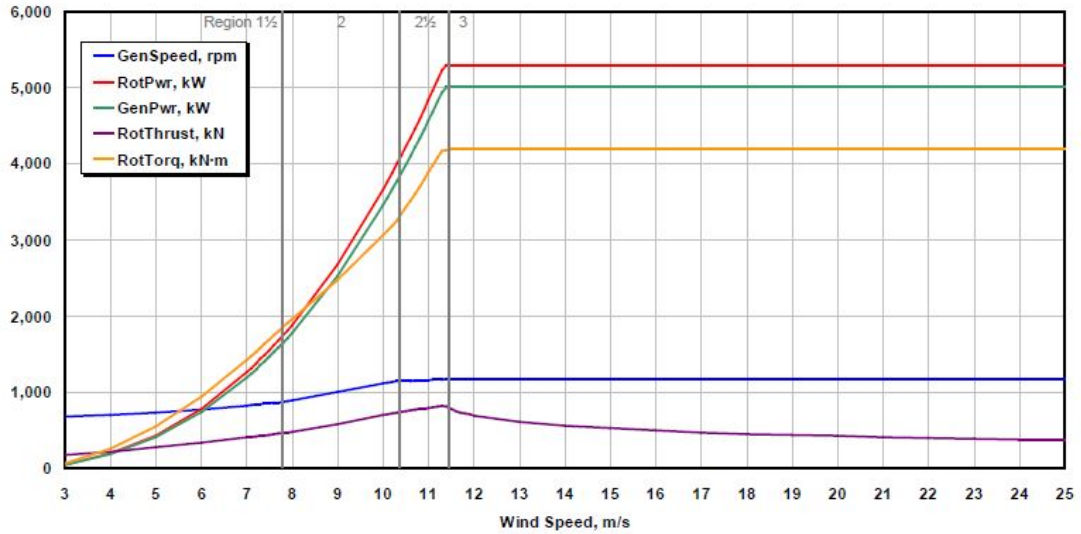
Figure 9.2: Thrust and torque curves for the rotor [14]

9.2 Support structure

Foundation

The foundation is a bucket foundation where the pressure from the earth on the bucket and the vertical bearing of the bucket provides stability against the overturning moment. The diameter of the skirt is 20 meters and the height of the bucket is 14 meters. Stiffeners are attached between the skirt and the transition peace to provide sufficient support. The foundation is implemented as a FEM model with soil properties. The soil properties are described below in Section 9.3.

Transition piece

The real transition piece design is shown in figure 9.4. It has a length of 65 meters. The diameter at the bottom where it is connected to the bucket is 8 meters and the diameter at the shaft towards the tower is 6 meters. The inner diameter of the grout is 5.84 meters as shown in the figure.

In the model the transition peace has a diameter of 8 meters at the base where it is connected to the bucket and a thickness of approximately 0.86 meters. In the FEDEM model the transition piece is modelled with a conical shape to preserve the physical properties of the grouting. The transition piece is modelled as a beam model where each beam has a length of 0.5 meters and a total of 130 beams. The cross section of each element is different to represent the grouting of the real transition peace.

Tower

The tower has a constant radius of 5 meters and thickness of 0.1 meters. The height of the tower is 75.1 meters. The tower is modelled as a beam structure with 5 beams of length 0.2 meters at the bottom and 5 beams of length 13.02 meters at the top.
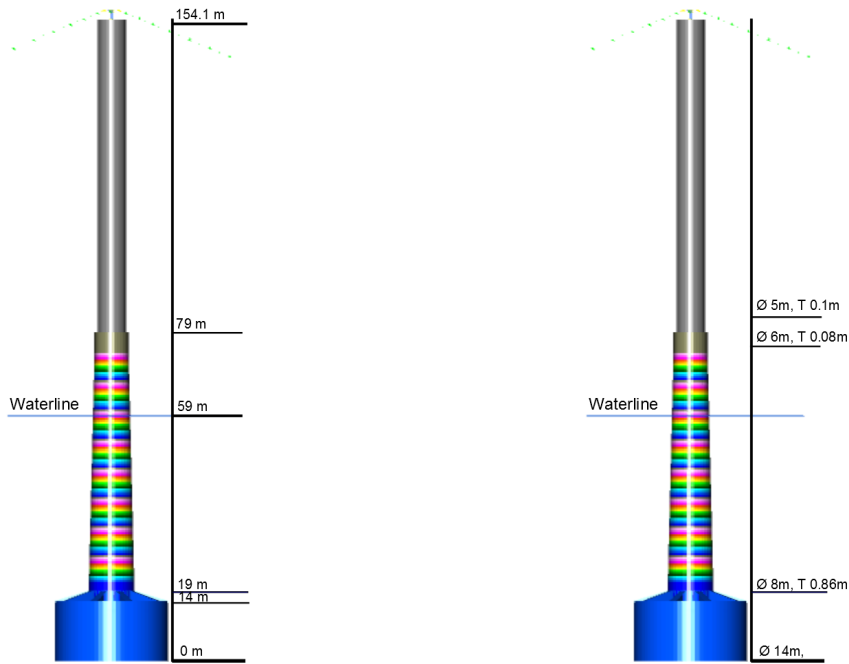
(a) Length dimension of structure

(b) Diameter and thickness of structure

Figure 9.3: Dimensions of supporting structure
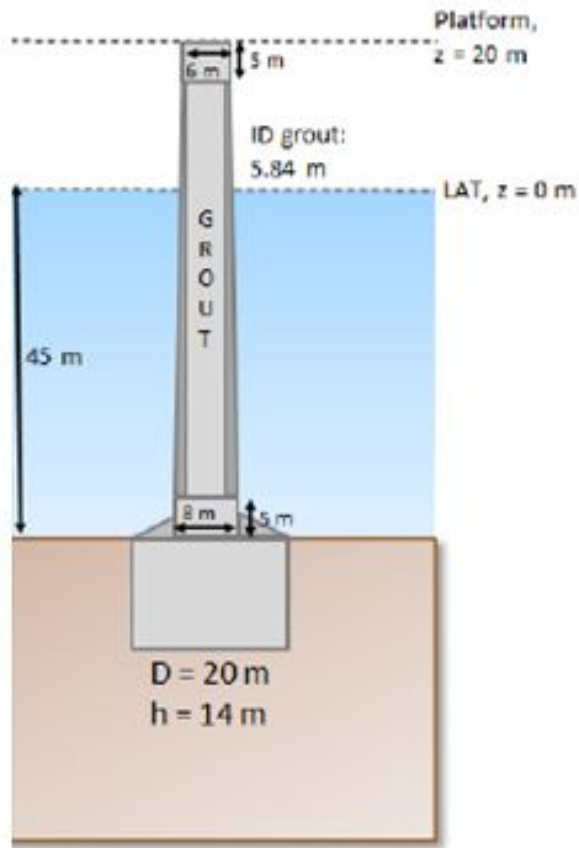
Figure 9.4: Dimension of foundation and transition piece

9.3 Soil Model

A soil model is implemented to represent the soil conditions around the bucket. This is to correctly model the stiffness of the earth around the bucket and get correctly stiffness properties to the eigen-value analysis and time domain analysis in FEDEM. The soil model is a FEM model where the physical properties of the soil are preserved in the model. The diameter of the soil model is 72 meters. The top 3 meters represent medium dense sand and then there is clay down to 40 meters depth. A 3D-perspective of the model is shown in Figure 9.5.

Both layers are modelled with a static and dynamic elastic module. The statical elastic module represent stress-to-strain ratio in case of large displacement and the dynamic elastic modules represent vibration with small displacement. The properties of the soil is related to offshore geotechnical engineering and will not be further described here. The soil parameters are listed in Table 8.

The soil conditions are often implemented with a multi dimensional non-linear stiffness spring. Multi dimensional meaning that the spring has a stiffness in x, y and z-direction. Also rotational stiffness is implemented. One benefit with the FEM soil model is that you can implement separate damping and stiffness in the soil and the steel construction. Also, non-linear springs my be difficult to implement. The vibration from the buckets can also be damped out in the soil model.

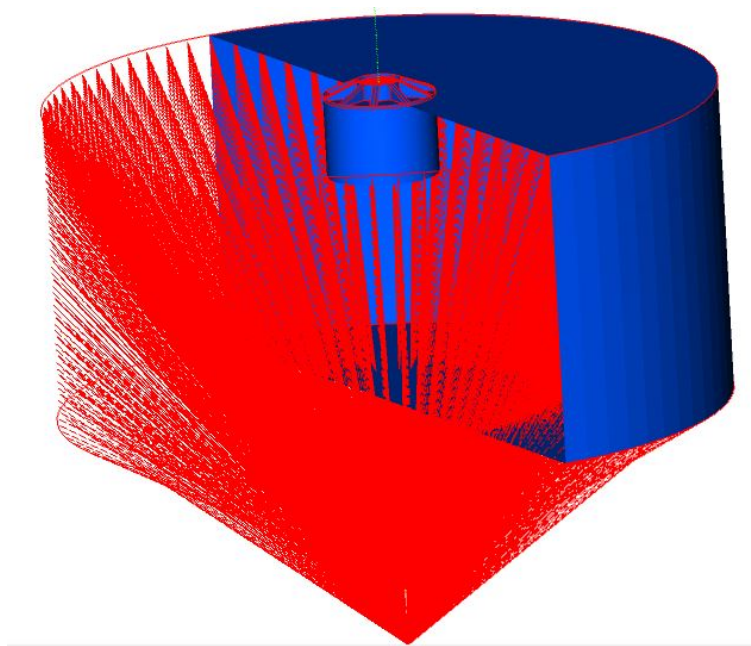| Elevation below mud line [m]	Soil type [-]	Eff. weight [kN/m³]	Undr. Shear strength [kPa]	Internal friction Φ[°C]	Cohesion C [kPa]	CPT cone resistance [MPa]		E_dyn [kN/m²]	E_stat [kN/m²]
						Top	Bottom		
0-3	Medium dense sand	10.0	-	37	0	0.0	7.5	69 000	34 500
3-40	Clay Till	10.0	250	-	-	5.0	5.0	188 000	37 600

Table 8: Soil properties

Figure 9.5: 3D-perspective of the FEM soil model

10 Eigen-Value Analysis

One of the major design criteria for an offshore wind turbine is the natural periods and the corresponding eigen-modes of the structure. If eigen-periods of the structure are close to the periods of environmental loads, the structure has a higher probability of resonance. Resonance is when the structure oscillate at the same frequency as the environmental loads which will cause a considerable higher deflection of the structure. Resonant behaviour will cause great damage to the structure, especially in long term considerations. Some of the eigen-modes will have strong effects on the fatigue damage on the foundation.

Eigen-modes and eigen-periods is an inherent character of a structure. As described in section 7.1.1 and 7.1.2 the eigen-periods is only determined by the mass distribution and equivalent stiffness of the structure. To avoid resonant behaviour in the structure, the designers should ensure that the eigen-periods of the structure is far enough away from the environmental loads periods.

10.1 Natural frequency analysis in FEDEM Windpower

Natural frequency analysis is an important part of the vibration analysis. It is important to identify the eigen-modes where the structure is in danger to oscillate at resonant frequency. The natural frequency analysis is done in FEDEM Windpower. Eigen-value analysis is performed for the whole model including blades, tower, transition piece and bucket foundation. The number of eigen-modes included can be defined in the dynamic solver as shown in Figure 10.1.
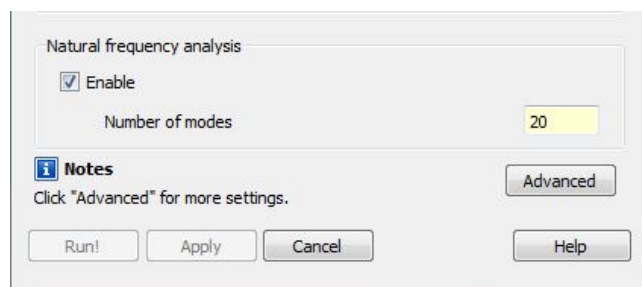
Figure 10.1: Natural frequency analysis

As described earlier it is possible to calculate as many eigen-modes as there are degrees of freedom in the system. Usually, there are only a number of eigen-modes that needs to be identified. The user needs to identify which natural frequencies are important and choose the desired number of modes to be calculated. A total of 20 modes was calculated and the results are listed in Table 9. The eigen-periods are given in Hz.

Table 9: Eigen periods of structure in Hz

Eigen-mode	Eigen-period	Eigen-mode	Eigen-period
1$^{\text{st}}$	0.24974	11$^{\text{th}}$	1.12027
2$^{\text{nd}}$	0.24982	12$^{\text{th}}$	1.19421
3$^{\text{rd}}$	0.65458	13$^{\text{th}}$	1.19662
4$^{\text{th}}$	0.65811	14$^{\text{th}}$	1.32519
5$^{\text{th}}$	0.67210	15$^{\text{th}}$	1.39103
6$^{\text{th}}$	0.86306	16$^{\text{th}}$	1.39413
7$^{\text{th}}$	0.91276	17$^{\text{th}}$	1.60553
8$^{\text{th}}$	1.04815	18$^{\text{th}}$	1.60554
9$^{\text{th}}$	1.07298	19$^{\text{th}}$	1.84979
10$^{\text{th}}$	1.09050	20$^{\text{th}}$	1.89774

From table 9 we can see all the eigen-modes and their belonging period. We can observe that the first and second bending mode is between the 1P and 3P frequency band which is 0.115 - 0.2 Hz and 0.345 - 0.6 Hz.

The solver will calculate the eigen-modes and their belonging periods, but it is up to the user to identify which mode is calculated. FEDEM gives the user the option to visualize the modes calculated in form of an animation. This is shown in Figure 10.2.
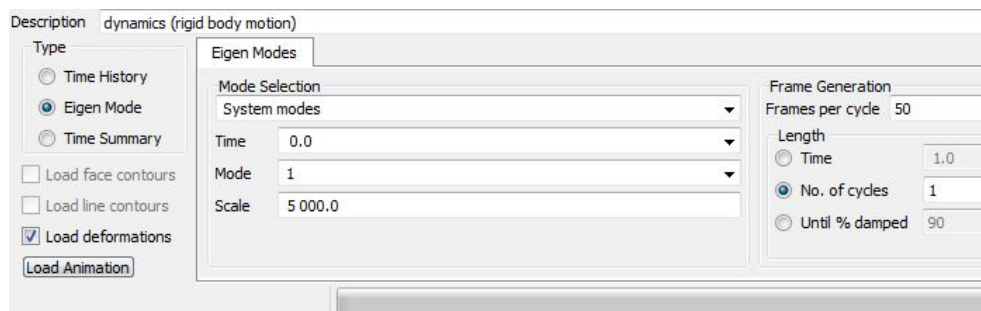
Figure 10.2: Identify eigen-modes

When considering the supporting structure, only a number of modes are of interest. The most important are 1$^{\text{st}}$ global fore-aft, 1$^{\text{st}}$ global side-to-side, 2$^{\text{nd}}$ global fore-aft and 2$^{\text{nd}}$ global side-to-side. The four modes of interest are shown below in figure 10.3 and 10.4. A scale of 10 000 is used to amplify the displacement of the support structure. This clearly affects the displacement of the blades as we can see for the second global fore-aft and second global side-to-side mode which are scaled out of proportion.

(a) 1st global fore-aft eigen-mode

(b) 1st global side-to-side eigen-mode
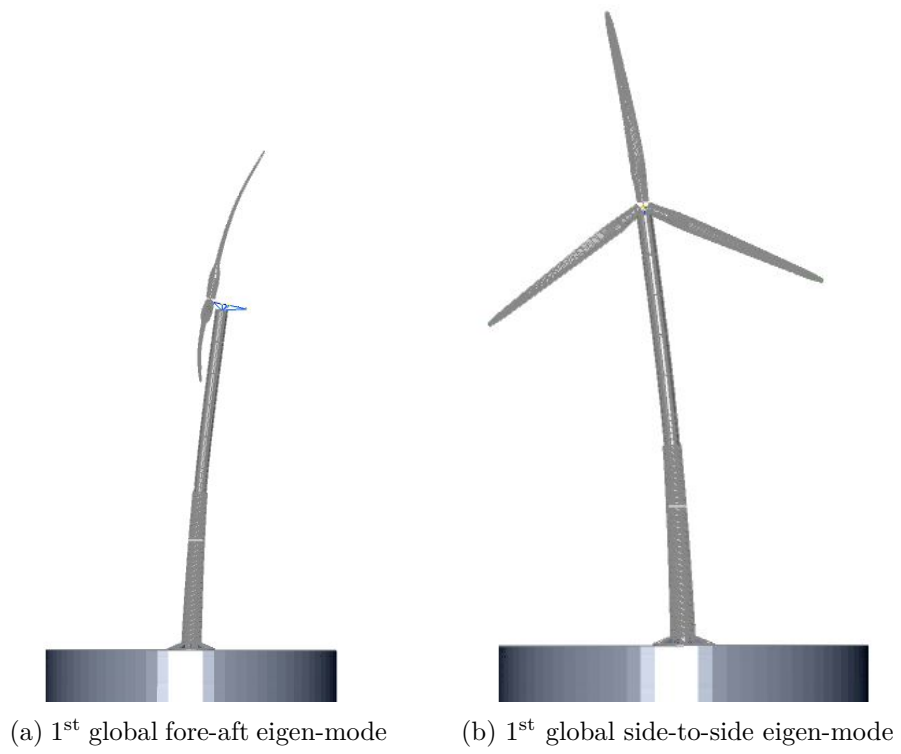
Figure 10.3: 1st and 2nd eigen-mode of structure

(a) 2nd global fore-aft eigen-mode

(b) 2nd global side-to-side eigen-mode
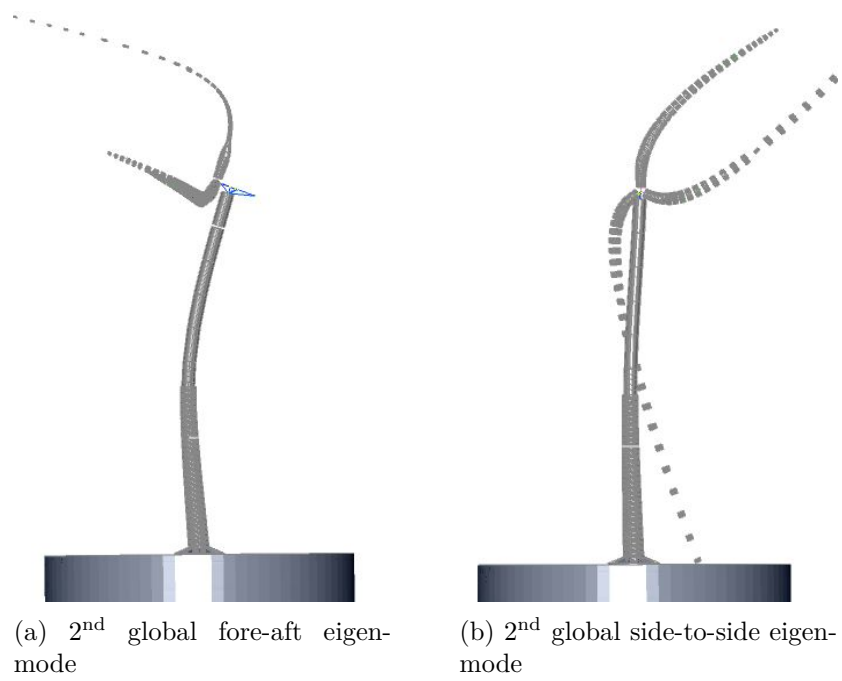
Figure 10.4: 7th and 8th eigen-mode of structure

The four modes of interest are identified as the 1st, 2nd, 7th and 8th eigen-modes. The 1st fore-aft eigen-mode is when the turbine has a deflection in the x-direction. We can see that the top of the tower moves in the x-direction and the blades has the same direction of deflection as the tower. The 1st side-to-side eigen-mode has the same characteristics as the fore-aft but deflects along the y-axis. The 2nd fore-aft eigen-mode is when tower bends in the x-direction around its middle. The blades will have the same direction of deflection as the middle of the tower, but opposite direction of the nacelle. The 2nd side-to-side mode have the same characteristics as the fore-aft and deflects around the y-direction.

The relevant eigen-modes of the structure and its belonging periods is listed in table 10.

Table 10: Eigen periods of structure in Hz

Eigen-mode	Eigen-period
1st fore-aft	0.249745
1st side-to-side	0.249829
2nd fore-aft	0.912769
2nd side-to-side	1.04815

10.2   Natural frequencies for larger turbines

Larger turbines will increase the top mass considerably. The weight of the blades will scale with a factor of 3 from simple theory. The rotor itself will also be attached further away from the tower. This is necessary as the deflection of the blades will increase for larger blades. Increasing the distance to the tower will change the radius of inertia from the tower. To simulate the effects of larger rotor, the mass of the hub is increased. To catch the effect of increasing the distance from the tower, the rotor is moved further away from the tower.

The ICORASS Feasibility Study present a study on very large wind turbines [3]. The study is for a 10MW turbine with blade length of 85m. Increasing the blade length from 63m to 85m, means that the tower has to be 22 meters longer. Changing the mass of the rotor can be done by the following scaling:

$$SF = \frac{85}{63} \approx 1.35$$

The new rotor mass will become:

$$\text{Rotor mass} = 110000 * 1.35^3 \approx 270000 kg$$

By only increasing the top mass of the structure, the natural frequencies will decrease for the structure. The results are given in Table 11. Increasing the rotor mass by 160 000 kilos does not make a considerably large effect to the natural frequency of the structure. The eigen-frequencies for the first fore-aft and side-to-side decreases with about 0.02Hz.

Also the second fore-aft bending mode decreases with 0.02Hz. The second side-to-side bending mode is almost unaffected.

Table 11: Eigen periods of structure with increased rotor mass in Hz

Eigen-mode	Eigen-period
1st fore-aft	0.22659
1st side-to-side	0.226663
2nd fore-aft	0.88104
2nd side-to-side	1.04422

In addition to increasing the top mass, the distance from the tower is increased with 10m to see how this effects the natural periods of the structure. The results are listed in Table 12. For the first fore-aft and side-side eigen-mode the changes are minimal. For the second fore-aft and side-to-side eigen-mode the changes are about 0.02Hz for both. The distance from the tower will influence the second bending mode, but not considerably. For larger rotor is seems like the length of the tower and changes in stiffness will have the biggest influence on the eigen-frequencies.

Table 12: Eigen periods of structure with increased rotor mass and distance from tower in Hz

Eigen-mode	Eigen-period
1st fore-aft	0.22448
1st side-to-side	0.22480
2nd fore-aft	0.86067
2nd side-to-side	0.98413

The length of the tower is also increased by 22m to adjust for the clearance of the longer blades to the water. The diameter and thickness of the tower is not changed. The first fore-aft and side-to-side eigen-frequencies are reduced by 0.3Hz. The second fore-aft bending-mode has decreased its eigen-frequency with 0.06Hz while the second side-to-side eigen-mode has increased by 0.016Hz.

Table 13: Eigen periods of structure with increased rotor mass, distance from tower and tower length in Hz

Eigen-mode	Eigen-period
1st fore-aft	0.194721
1st side-to-side	0.19485
2nd fore-aft	0.79504
2nd side-to-side	1.00378

11 Constant wind analysis

An analysis with only shear wind was performed to confirm that the shear wind profile itself will cause a peak in the power spectrum at the rotational frequency of the turbine. As described in Section 8.1, a blade passing through an eddy of higher wind speed than the mean wind speed will cause a load peak at the 1P frequency. In the same way, the shear profile itself without turbulent wind will cause higher wind speeds with increasing distance from the ground. When the blade passes over the turbine, each strip on the blade will experience a load peak.

Two load cases where tested. A constant wind of 8 m/s at the hub height which is below rated, and a mean wind speed of 14 m/s which is above rated for the turbine. Since there are no turbulence present in the simulation, the simulation time was no more than 10 minutes. This is not a problem as there are no statistical parameters to consider from wind and waves. Simulation parameters are listed in Table 14.

Table 14: Simulation parameters for constant wind speed

Load case 1	8 m/s constant wind
Load case 2	14 m/s constant wind
Simulation time	600 s
Time step dynamic solver	0.025 s
Time step AeroDyn	0.03 s
Radius for force calculation	1.55, 15.88, 36.36 and 50.7 m

11.1 Load case 1: Wind speed of 8m/s

For the load case 1 of wind speed 8 m/s, the rotational frequency of the blades are about 9.2 rpm or 0.153 Hz. Figure 11.1 shows the resulting power spectrum for the calculated aerodynamic forces on the different radius given in Table 14. The spectrum is calculated in FEDEM by using its internal Fourier Transform of the time series. This is to verify the shape of the power spectrum calculated in MATLAB. It is almost flat, but have a large sharp peak at the 1P rotational frequency of 0.153 Hz as shown in Figure 11.1. The time series is exported from FEDEM and the power spectrum is calculated in MATLAB. The resulting power spectrum is showed in figure 11.2 and we can see that is has the same shape. In figure 11.3 we have a closer picture of the peak. Even though the peak is very high, it is very sharp and the bandwidth is small. The longer the bandwidth is, the more it will contribute to fatigue damage. The figure also shows that the peak is larger closer to the rotor.
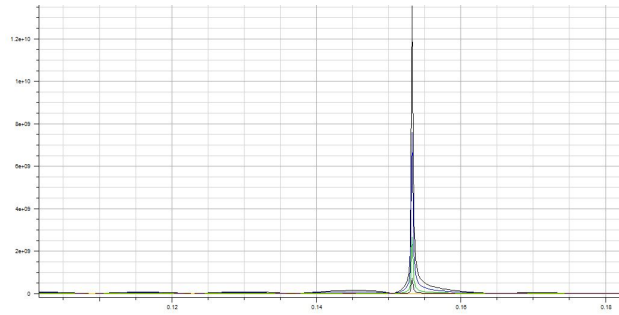
45

Figure 11.1: Power spectrum for different blade radius at constant wind 8 m/s
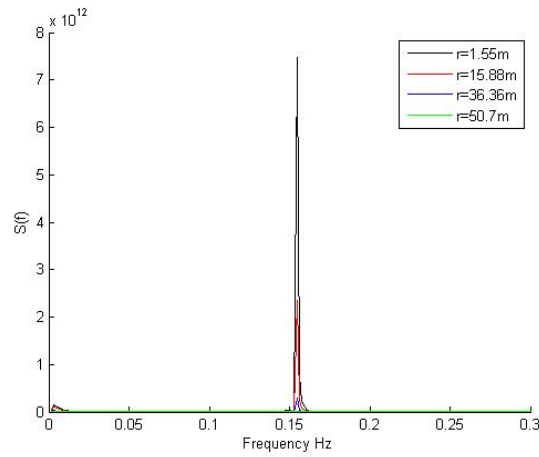

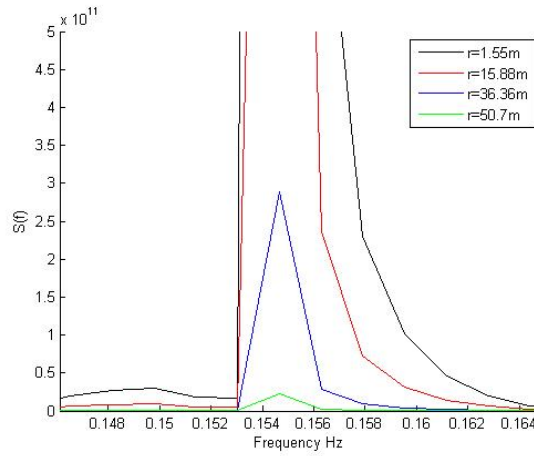Figure 11.2: Power spectrum for different blade radius at constant wind 8 m/s

Figure 11.3: Closer look at the peak for constant wind 8 m/s

11.2 Load case 2: Wind speed of 14m/s

For the load case 2 of wind speed 14 m/s, the rotational frequency of the blades are 12.1 rpm or 0.2 Hz. As for load case 1, the aerodynamic force on the same radius are calculated and plotted as a power spectrum. We can see that a large sharp peak appears at the 1P rotational frequency of 0.2 Hz. The blades experience a load peak each time the blade passes over the hub. The power spectrum is showed in figure 11.4. From the closer look in figure 11.5 we see that it has the same characteristics as for load case 1. The peak is higher for the inner diameter, and decreases further out on the blade.
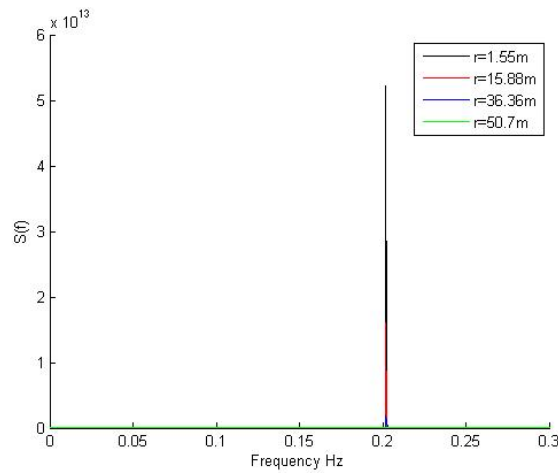

Figure 11.4: Power spectrum for different blade radius at constant wind 14 m/s
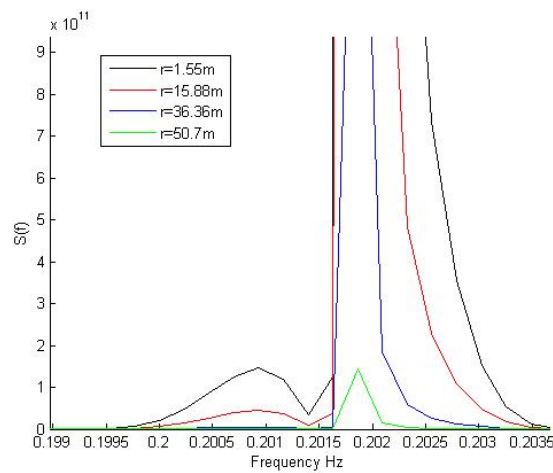

Figure 11.5: Closer look at peak for constant wind 14 m/s

11.3 Discussion

The analysis show that each blade will experience a load peak due to wind shear profile each time it passes over the hub. This is what is expected for a non turbulent wind, with increasing wind velocity from the ground. Load case 1 and 2 also shows that for a variable speed wind turbine the peak in the power spectrum will change its peak frequency with the rotational speed of the rotor. This is the reason why the 1$^{\text{st}}$ natural frequency of the foundation has to lie outside the frequency band of the 1P frequency and 3P frequency. In absence of turbulence, the blades will not experience any peaks in forces at other frequencies.

12 Setup for integrated analysis with turbulent wind and wave loads

12.1 General

Dynamic behaviour of offshore structures needs to consider environmental loads induced by waves, wind and currents. Compared with offshore oil and gas platforms, the wind loads are fare more significant than waves for an offshore wind turbine due to the dimension of the blades. It is necessary to estimate both aerodynamic and hydrodynamic loads accurately. The analysis of offshore wind turbines relies on aero-hydro-servo-elastic simulation codes [20]. These coupled time domain tools take into account an interaction of various environmental conditions and the entire structural assembly of the turbine. Also the control system of the turbine needs to be included which makes the analysis very complex.

There are several academic and commercial computer programs used for analysis of wind turbines where Bladed, FAST and HAWC2 are some examples. In this thesis, the combination of aerodynamic and hydrodynamic analysis is done in a coupled analysis. Fedem Windpower uses AeroDyn for calculation of the forces due to wind on the blade elements. AeroDyn bases its calculations on the input from the air environment, updated positions and velocities of the wind turbine and drag and lift coefficient. The output forces from Aerodyn is used by Fedems dynamic solver to provide results that can be analysed.

Time-domain simulations will be carried out in FEDEM to get the response and forces of the blades, tower and the foundation under wind and wave loads. The current is neglected under the assumption that it will not give a major contribution to the foundation. Results from time-domain simulation is exported an post processed in MATLAB where the results are transformed to power spectra in the frequency domain. As explained in Section 4, several characteristics responses can be distinguished from a power spectrum compared to a time series. The simulation and post-processing is quite time consuming work due to the lack of heavy computer power. The time increment in the dynamic solver have to be very small to get accurate results.

12.2 Environmental conditions

12.2.1 Wind Conditions

The wind conditions considered in this thesis is a mean wind speed ranging from 2 m/s and up to 18 m/s with an increment of 2 m/s. The mean wind speed are at reference height of 10 meters, meaning that the wind speed at the hub will be higher according to the wind profile described in Section 6.2. At the hub height this will correspond to a wind speed ranging from just above cut-in speed of 3 m/s and just below cut-out speed of 25 m/s. Under the assumption that the response in the blades at operational conditions will propagate down to the foundation, extreme wind conditions where the

49

turbine is shut down will not be considered.

Turbulent wind is applied and is based on the IEC Kaimal wind spectrum with the mean wind speed as described above. The turbulence intensity is IEC class A, which correspond to a turbulence intensity of 18%. The turbulence intensity, I, is defined as

$$I = \frac{\sigma}{V_{10min}}$$

where V_{10min} is the mean wind speed within a 10 minute interval and σ is the standard deviation of the wind speed within the same time interval.

Table 15: Wind conditions for simulations

Mean wind speed at reference height 10 m	2 m/s to 18 m/s
Turbulence intensity	18 %

12.2.2 Wave conditions

The wave conditions are chosen from site conditions at Dudgeon, 32km off the cost of the seaside town Cromer in North Norfolk, England. The wave conditions are chosen as the most likely waves to occur at different wind speeds. Data are taken from the NORA10 database [21]. With a wind speed of 8 m/s the most likely waves to occur have $H_S = 1m$ and $T_P = 5s$. At the highest wind speed of 18 m/s, the most likely waves to occur have $H_S = 3m$ and $T_P = 7s$. The direction of the waves will be zero degrees, meaning that the waves will have the same direction as the wind for all the simulation. All the wave conditions are listed in table 16.

Table 16: Wave conditions for simulations

H_S [m]	T_P [s]
1	5
2	6
3	7

12.3 Time-domain Simulations

The dynamic behaviour for the offshore wind turbine is performed in time-domain. As mentioned previously in section 12.1, the analysis is done decoupled. Fedem calls upon AeroDyn code for calculations of the forces due to wind on the blade elements. Aerodyn bases its calculations on the input wind-file created in TURBSIM. For the turbulent wind load, the blade momentum theory (BEM) with skewed wake and tip loss correction is used. This is an iterative method which assumes that the wake is always in equilibrium with the forces on the blade [1].
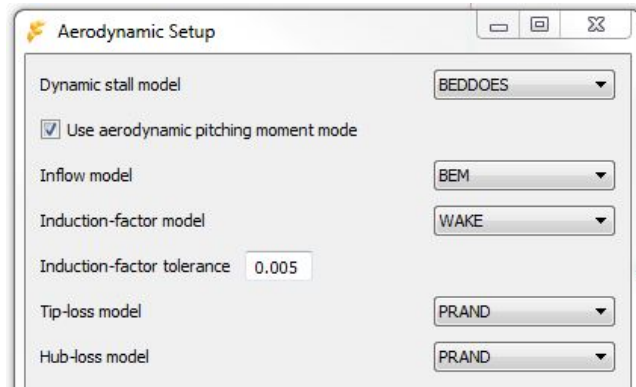
Figure 12.1: Aerodynamic setup in FEDEM

The wave loads are computed based on Morison equation. The wave loads includes the drag and added mass loads around the cylinder. Each simulation is run for 3600 s. Since wind is considered stationary for 10 minutes, this means that we have 6 simulations where the wind is considered stationary.

12.3.1 Time step in analysis

A sensitivity in the time step was performed to ensure the most correct results from the simulations. The time step is important for this coupled simulation, especially because of the way the blades passes the three-dimensional wind velocity field. A two-dimensional plane of the wind field is shown in figure 12.2. The cross section shows that the wind field consist of a grid of vectors in the yz-plane. Each vector have the U, V and W wind velocity, corresponding the velocity in each direction. When AeroDyn calculates the forces on the blades it will have to interpolate between these vectors. Since the turbine is rotating very fast, the time step have to be very small to catch the effects from the turbulent field.

When using the same time step in the dynamic solver and the aerodynamic calculations there where sometimes numerical instabilities. The solution do not converge and the simulation would stop at some point. Since the time integration steps in the numerical solver (dt) often are quite small, the dynamic simulations can run faster and be more immune to numerical stability problems if the time step for aerodynamic solver (dtAD) is specified larger than dt, but still less than the time scale for the changes in aerodynamic forces [1]. The aerodynamic forces are not expected to change faster than the time it takes the turbine to rotate 2.4°. For the rated speed of 12.1 rpm, this correspond to 0.03 s. This means that the aerodynamic time step should be 0.03 seconds or smaller. The dynamic solver time step should also be smaller than the aerodynamic time step. When defining the NREL 5MW reference turbine, Jonkman et al. found that the highest time steps for numerical stability was 0.025s for AeroDyn while using 0.0125s for the dynamic solver [14]. Still they used other software for dynamic calculations.

The time step was chosen to be 0.025 for AeroDyn and 0.0125s for the dynamic solver. This time step seemed to catch the aerodynamic forces best. It was not possible to choose lower time steps due to lack of computer power.
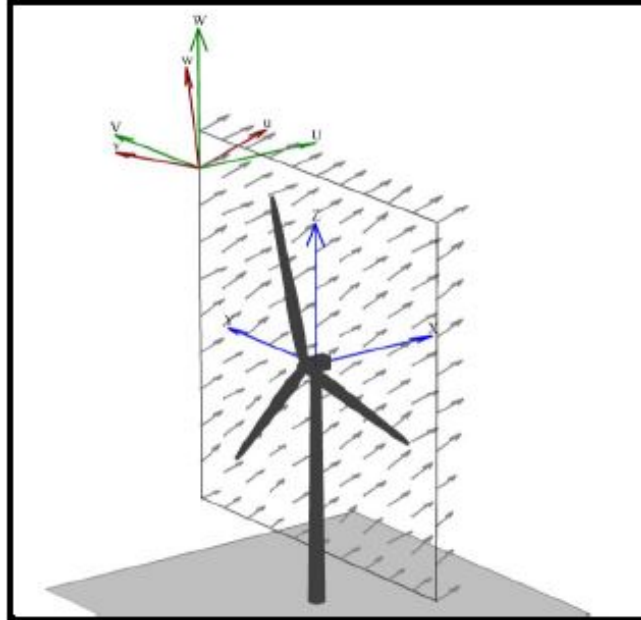

Figure 12.2: Two-dimensional cross section of the three-dimensional wind field [13]

12.4 Post processing

The post processing is done in MATALB. The results from the time-domain simulations are exported as text files. The results are transformed from time series to the frequency domain by use of Fast Fourier Transform algorithms as explained in section 4.2. The technique of Windowing with 50% overlap is used on the time series. Each time series of 1 hour is split into 6 windows of 10 minutes which is the time wind is considered stationary. With a 50% overlap this gives a total of 11 windows. The resulting power spectrum is an average of the 11 windows.

13 Blade forces and response with wind and waves

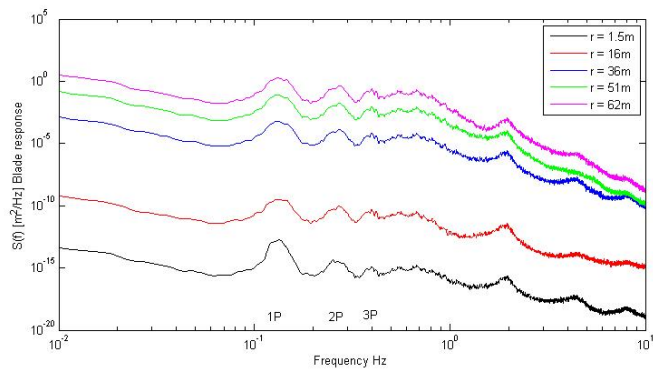## 13.1 Low wind speeds 3 - 8m/s at hub height

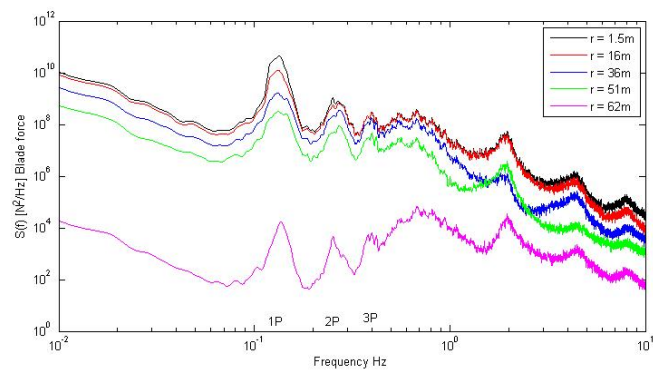Figure 13.1: Log-log blade response, HS=1m TP=5s U=5.5m/s

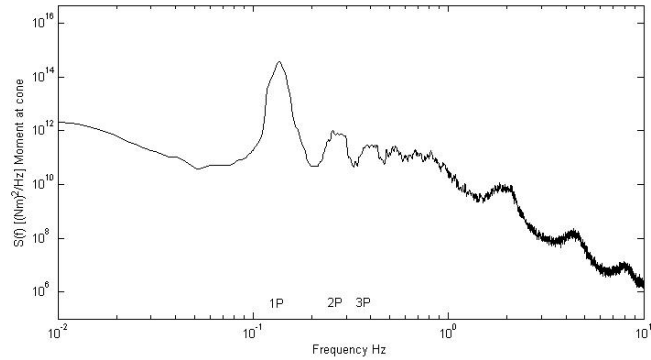Figure 13.2: Log-log blade force, HS=1m TP=5s U=5.5m/s

Figure 13.3: Log-log moment at cone, HS=1m TP=5s U=5.5m/s

Figure 13.1 shows the power spectrum for the blade response or deflection of the blades for the load case $H_S = 1$m, $T_P = 5$s and mean wind speed $U_{hub} = 5.5$m/s. We can distinguish a peak at the 1P, 2P and 3P rotational frequency for all the strips on the blade. Except for these three peaks there are few clear peaks, except around higher frequencies like 2Hz and 4Hz. The peaks are not very sharp, but have a very thick tail, meaning that the bandwidth is large. We can see that the response increases with the blade length.

The force on the blade in the wind direction is shown in figure 13.2. The force decreases further away from the hub. We can clearly see a peak 1P, 2P and 3P. Each strip on the blade reaches the highest force as it passes over the top of the tower. It is expected that there will be an increase in force at the rotational frequency.

Figure 13.3 shows the power spectrum of the integrated force along the blade. The integrated force is taken as the moment at the cone where the blade is attached to the hub. The shape of the curve is very similar to that of the force on the blades. This shows that the force on each strip on the blade is highly correlated.

The three figures above is very similar for all the load cases where the wind is 3m/s to 8m/s at hub height. The shape of the spectrum describes the response and forces on the blades for low wind speeds.

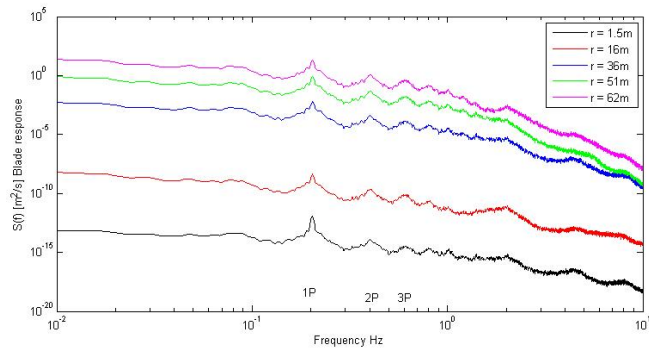## 13.2 Medium wind speed 11 - 14m/s at hub height

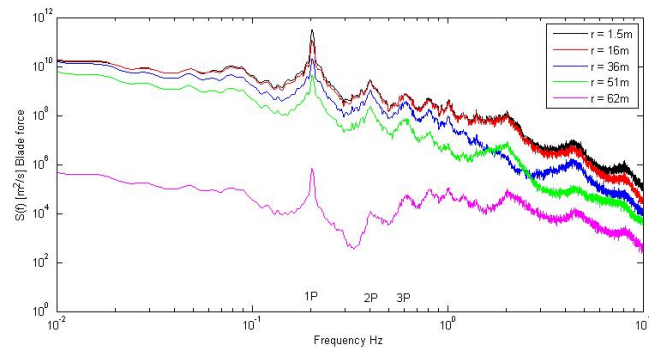Figure 13.4: Log-log blade response, HS=1m TP=5s U=14m/s

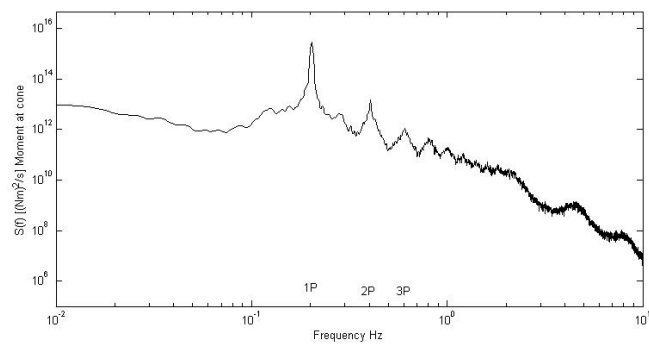Figure 13.5: Log-log blade drag force, HS=1m TP=5s U=14m/s

Figure 13.6: Log-log moment at cone, HS=1m TP=5s U=14m/s

Figure 13.4 shows the power spectrum for the blade response or deflection for the load case $H_S = 1$m, $T_P = 5$s and mean wind speed $U_{hub} = 14$m/s. Compared to low wind speeds we can also see small peaks at 4P and 5P, even though they are small. The responses are generally higher for all frequencies compared to low wind speeds.

The force on the blade in the wind direction is shown in figure 13.5. The peaks in the spectrum are sharper compared to low wind speeds. For low wind speed we saw peaks at 1P, 2P and 3P. Here we can also distinguish peaks at 4P, 5P and 6P. The forces are highest closest to the hub and decreasing further out on the blade.

Figure 13.6 shows the power spectrum of the integrated force along the blade and is taken as the moment at the cone. Compared to low wind speeds the peaks are sharper and we can easily distinguish peaks at 1P, 2P, 3P, 4P, 5P and 6P. The forces from each strip of the blade is highly correlated as the integrated force have the same shape.

The three figures above is very similar for most of the load cases where the wind is 11m/s to 14m/s. However, for medium wind speeds there were also a load case where the peaks in the power spectrum was very sharp.
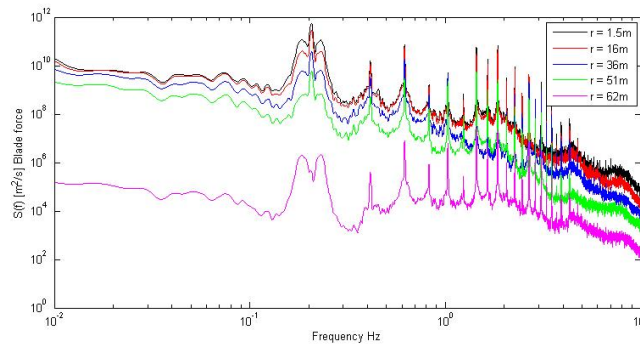

Figure 13.7: Log-log blade forces, HS=2m TP=6s U=11.1m/s

Figure 13.7 shows the power spectrum for the forces on the same strips of the blade for the load case $H_S = 2$m, $T_P = 6$s and mean wind speed $U_{Hub} = 11.1$m/s. Here we can see that there are large peaks around the rotational frequency and all its harmonics.

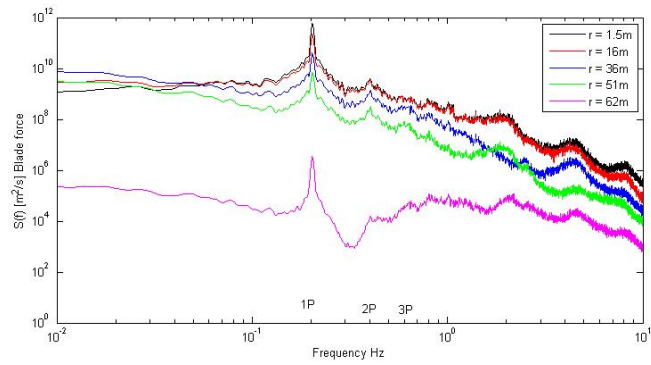## 13.3 High wind speeds 16 - 25m/s at hub height

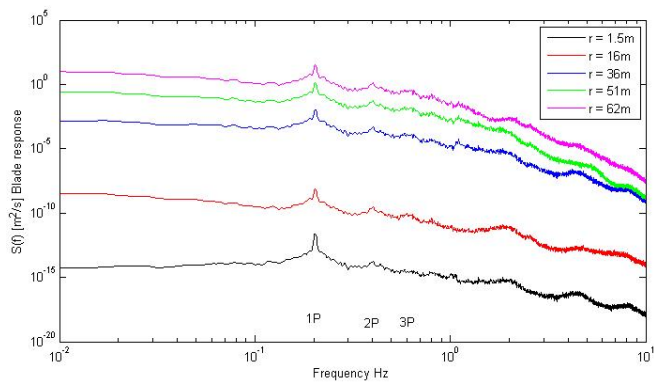Figure 13.8: Log-log blade response, HS=1m TP=5s U=22m/s

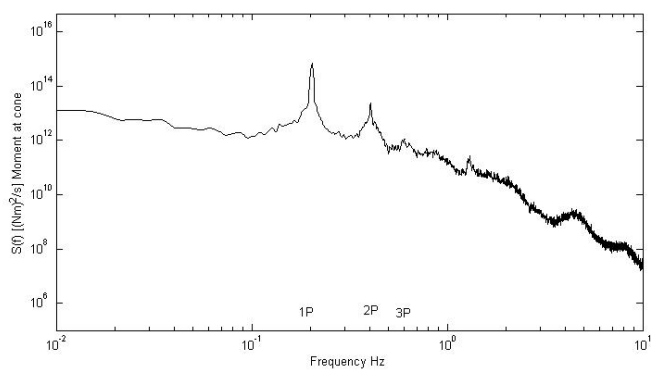Figure 13.9: Log-log blade drag force, HS=1m TP=5s U=22m/s

Figure 13.10: Log-log moment at cone, HS=1m TP=5s U=22m/s

Figure 13.8 shows the power spectrum for the blade response or deflection for the load case $H_S = 1$m, $T_P = 5$s and mean wind speed $U_{hub} = 22$m/s. We can distinguish a large sharp peak at the rotational frequency of 1P. Except for this large peak there are few distinguished peaks below 1Hz. We can see a peak at 2P which is small.

The force on the blade in the wind direction is shown in figure 13.9. The peak at the rotational frequency is clear. The peaks at higher frequencies are almost vanished compared to medium wins speeds.

Figure 13.10 shows the power spectrum of the integrated force along the blade. For the integrated force we can distinguish peaks at 1P, 2P, 3P and 6P. The forces on each strip of the blade is still highly correlated.

13.4 Discussion

The results from the simulation are very similar of the results found by Tcherniak et al. [24]. They found that the wind speed fluctuations at the blades have peaks at the rotational frequency and its harmonics. From the results of the simulations, the following observations can be made:

- The spectra for force and response have peaks at the rotational frequency and its harmonics.

- The shape of the curve is very similar for all strips on the blade.

- The response increase with increasing radius

- The force decreases with increasing radius

- The response and forces on different radius of the blade are highly correlated.

For wind without turbulence we saw that the blades experience a load peak at the rotational frequency of the rotor. In a turbulent field the blades will experience a load peak and a response peek at rotational frequency and its higher harmonics. The model is a variable speed turbine, meaning that the rotational speed of the rotor will increase from cut-in wind and up to rated wind speed of 11.4 m/s. The peaks in the power spectrum in turbulent wind moves in the frequency domain with the rotational speed of the rotor.

When the wind speed is above rated the blades are pitched to reduce the the thrust force. From the thrust curve given in Figure 9.2 we can see that the thrust force increase to rated speed, then reduces for higher wind speeds as the blades are pitched. For low wind speeds we see that response and forces on each strip are generally lower than for higher

wind speeds. At rated wind speed where the trust force is at its highest we see very high distinctive peaks at the rotational frequency and all its higher harmonics. This is logical since the forces on the blades are highest around rated. For higher wind speeds the peaks are lower and we cannot clearly see the peaks above 3P.

The forces on each strip of the blade are highly correlated. The integrated force taken as the moment at the cone where the blades are attached to the hub, shows that the integrated force over the blade has the same shape in the power spectrum as the force on a strip. This has a direct consequence when the length of the blades increases. Since the force and response is correlated, the deflection of the blades will increase with longer blades giving a higher response. Also the total force over the blade and the moment at the cone will increase. This will have a direct influence on fatigue on the blades and tower. Larger response and forces that comes in cycles will increase the stresses in the structure and the fatigue life.

14 Forces and response in foundation

This section shows the main results in forces and response in the foundation from the simulations. The horizontal force, the moment and response will be presented. The first global fore-aft eigen-frequency will be referred to as the first natural frequency of structure and the second global fore-aft eigen-frequency will be referred to as second natural frequency of structure. The results are taken from the node in the mudline. Wind speeds are given at hub height.

The reader should notice that:

- First natural frequency of structure equals about 0.25 Hz

- Second natural frequency of structure equals about 0.91 Hz.

All plots for the horizontal force have the same scale on the x-axis and y-axis. There are peaks in the spectrum above the y-axis, but there is a need zoom in a little to catch the energy around the second bending mode. It is the same for moment and response.

14.1 Load case $H_S = 1m$, $T_P = 5s$

14.1.1 Wind at hub height = 5.5m/s

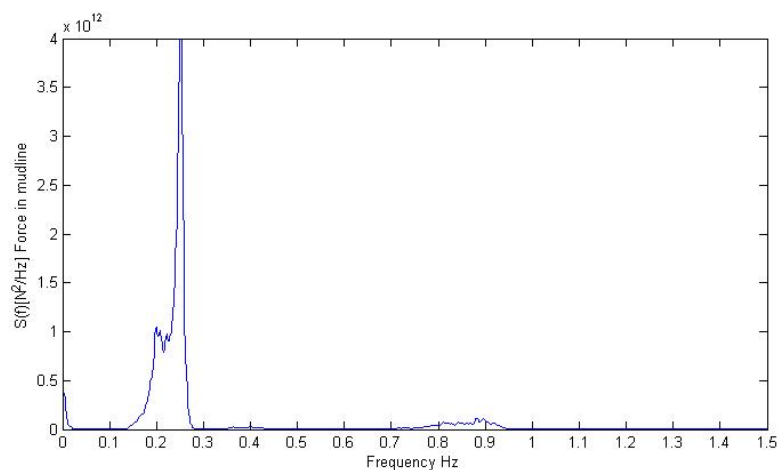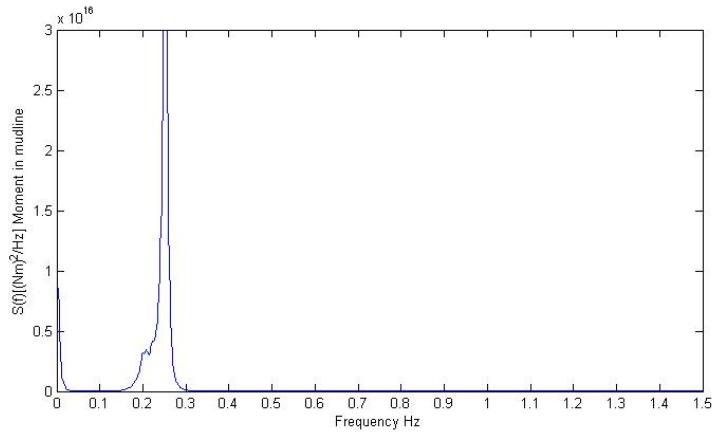Figure 14.1: Force mudline, HS=1m TP=5s U=5.5m/s

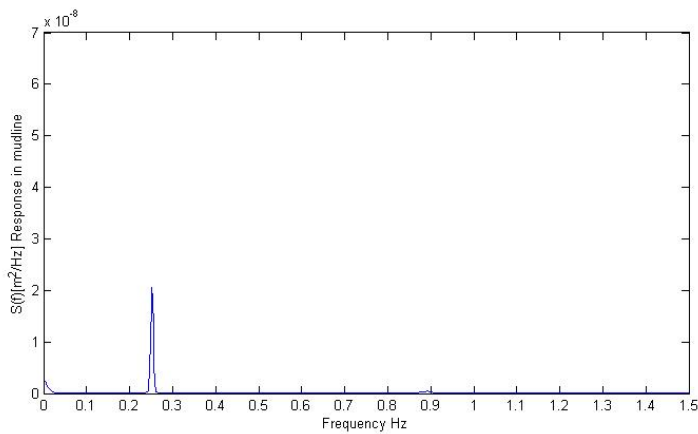Figure 14.2: Moment mudline, HS=1m TP=5s U=5.5m/s

Figure 14.3: Response mudline, HS=1m TP=5s U=5.5m/s

Figure 14.1 shows the power spectrum for the horizontal force in the mudline for the given load case. There is energy in the area from 0.1Hz to 0.3Hz. We can identify a small peak at 0.2Hz, which is the peak frequency of the waves and a much larger peak at the first natural frequency of the structure. There is also a small contribution around 0.9Hz which is the second natural frequency of the structure. However, it is barely visible.

Figure 14.2 shows the power spectrum for the moment in the mudline. Similar to the force the energy in the spectrum is between 0.1Hz and 0.3Hz. A large peak appears at the first natural frequency of the structure.

Figure 14.3 shows the power spectrum for the rotational response. There is a sharp, but small peak at the first natural frequency of the structure. Little or no energy at other frequencies.

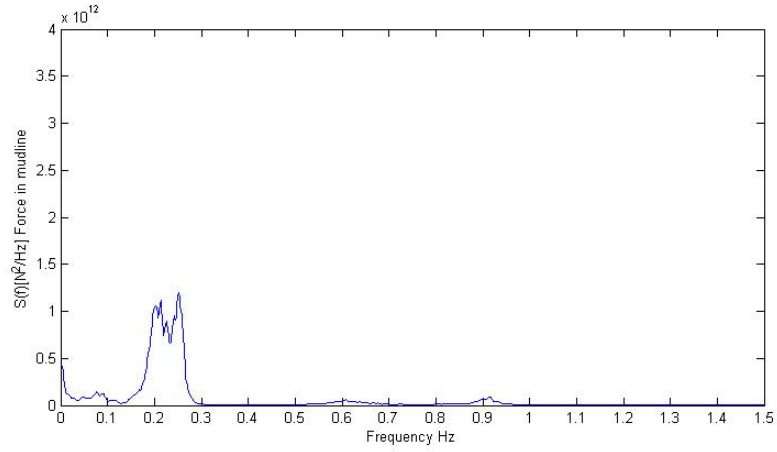## 14.1.2 Wind at hub height = 14 m/s

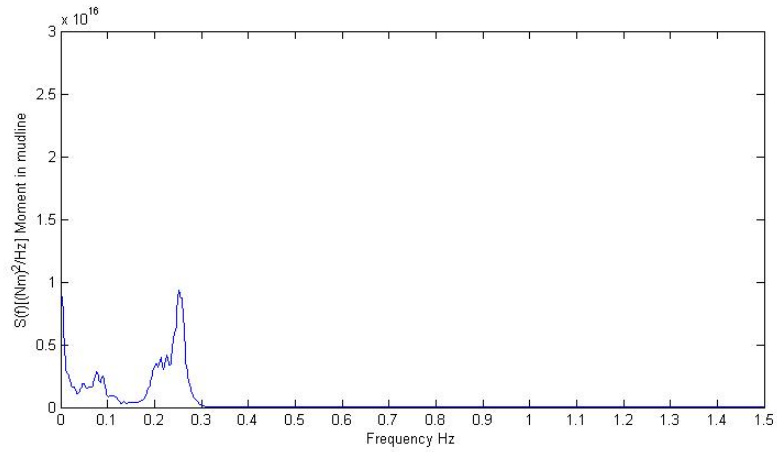Figure 14.4: Force mudline, HS=1m TP=5s U=14m/s

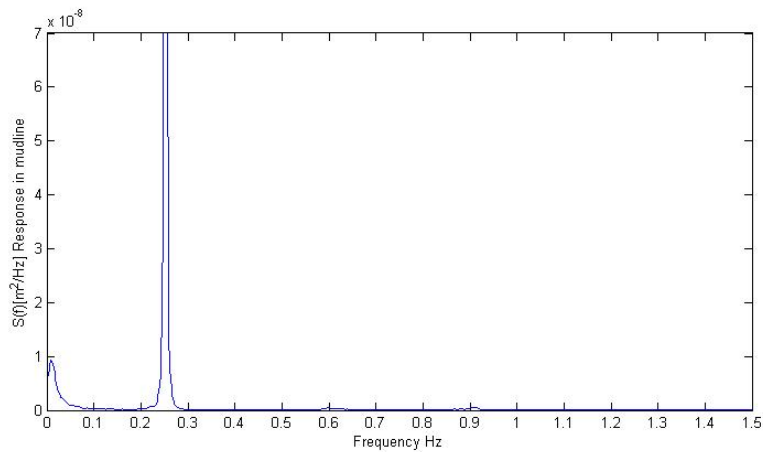Figure 14.5: Moment mudline, HS=1m TP=5s U=14m/s

Figure 14.6: Response mudline, HS=1m TP=5s U=14m/s

Figure 14.4 shows the resulting power spectrum of the horizontal force in mudline when the mean wind speed is increased to 14m/s. The blades are now pitched 8.7°. Compared to wind speed of 5.5 m/s the peak at the first natural frequency is much smaller. We can identify a small peak at 0,6Hz corresponding to 3P and around the second natural frequency of 0.91 Hz. More energy in the lowest frequencies where the shape of the curve is similar of the wind spectrum.

Figure 14.5 shows the power spectrum of the moment. Similar as the force, the peak at the first natural frequency is heavily reduced to more than half compared to the load case of mean wind speed of 5.5 m/s. Also more energy in the lower frequencies below 0.1 Hz.

The peak for the rotational response increases dramatically to almost three times its value compared to wind speed of 5.5m/s. This is shown in figure 14.6. The peak is at the first natural frequency of the structure. A very small peak appears around the second natural frequency of the structure. There is also more energy in the lower frequencies of the wind.

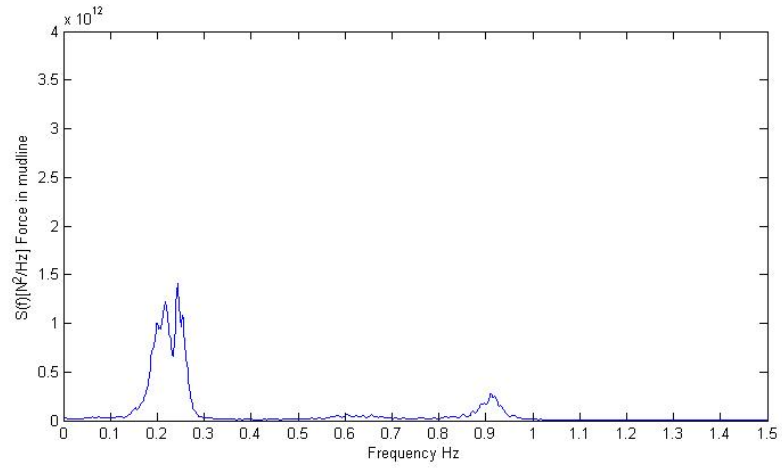### 14.1.3 Wind = 22 m/s

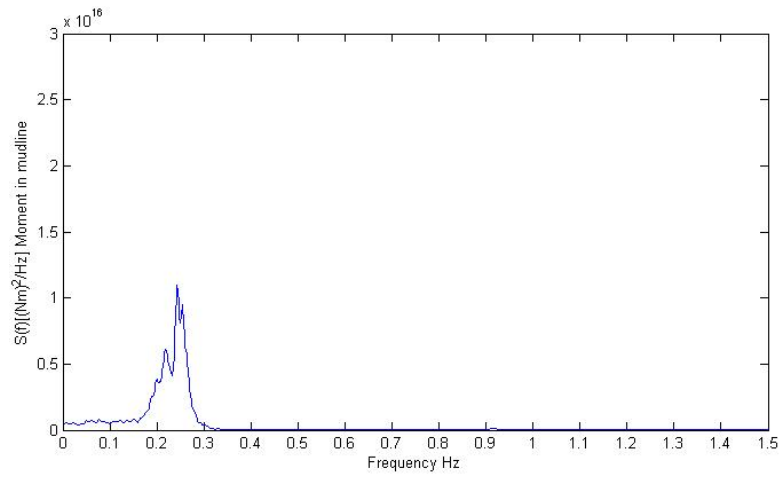Figure 14.7: Moment mudline, HS=1m TP=5s U=22m/s

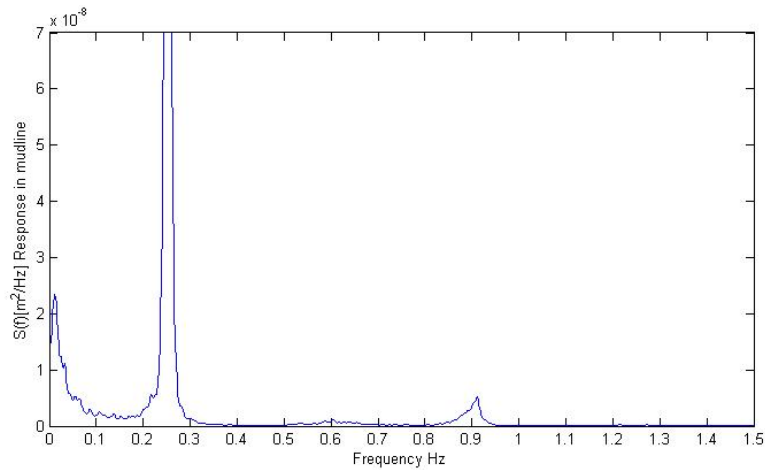Figure 14.8: Moment mudline, HS=1m TP=5s U=22m/s

Figure 14.9: Response mudline, HS=1m TP=5s U=22m/s

Figure 14.7 shows the power spectrum of the horizontal force in mudline when the wind speed at hub height is further increased to 22m/s. The shape of the curve is very similar to mean wins speed of 14m/s. A peak at the wave peak frequency of 0.2Hz and first natural frequency of the structure is identified. The peak at the second natural frequency of the structure is larger.

The power spectrum for the moment is shown in figure 14.8. The energy in the spectrum lies between 0 and 0.3 Hz. There is a peak at the wave peak frequency and a larger peak around the first natural frequency of the structure.

The response in the foundation is largest for the highest wind speed. Figure 14.9 shows the resulting power spectrum of the rotational response when the wind speed is increased to 22m/s. There is much more energy in the lower frequencies below 0.1 Hz. The peak at the first natural frequency has a much larger peak, and the bandwidth of the peak has increased. There peak at the second natural frequency of the structure at 0.91Hz is larger compared to wind speed of 14m/s.

14.2 Load case $H_S = 2m$, $T_P = 6s$
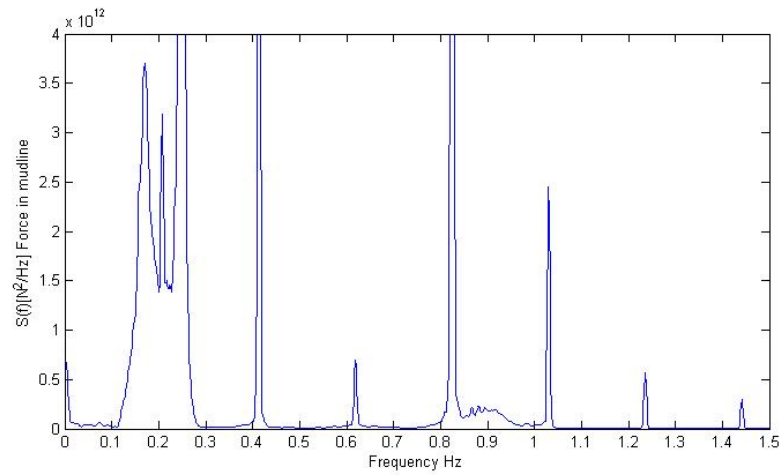
14.2.1 Wind at hub height = 11.1m/s
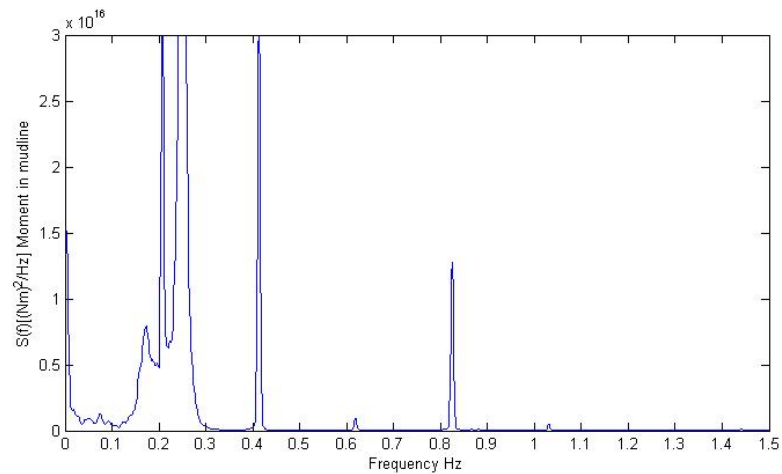

Figure 14.10: Force mudline, HS=2m TP=6s U=11.1m/s

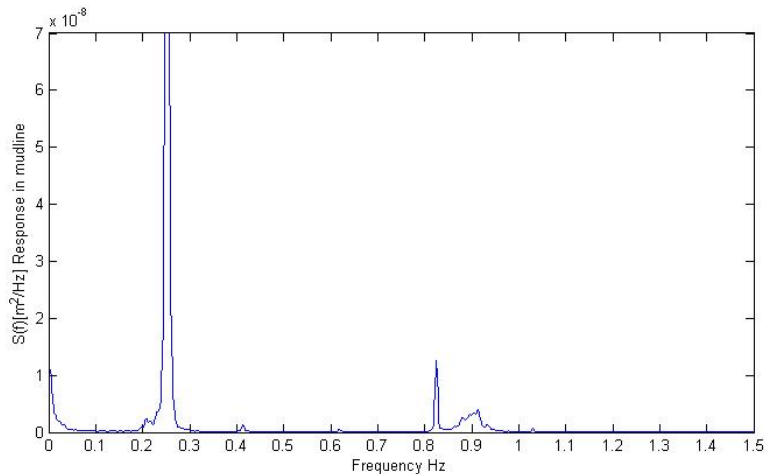Figure 14.11: Moment mudline, HS=2m TP=6s U=11.1m/s

Figure 14.12: Response, HS=2m TP=6s U=11.1m/s

A wind speed of 11.1m/s is very close to the rated wind speed of 11.4m/s. Figure 14.10 shows the resulting power spectrum for the horizontal force in the mudline. We can recognize the peak at the wave peak frequency and the first and second natural frequency. We can also identify peaks at at the rotational frequency 1P = 0.2Hz and all its harmonics. The peak at 0.4Hz and 0.8Hz are very sharp and high.

Figure 14.11 shows the power spectrum of the moment. There is a large sharp peak at the wave peak frequency of 0.16Hz and the first natural frequency of the structure. Compared to other load cases there is also sharp peaks at the rotational frequency and all its higher harmonics. At 2P and 4P corresponding to 0.4Hz and 0.8 Hz we have very large sharp peaks.

In the rotational response power spectrum in figure 14.12 we can identify the peaks at the first and second natural frequency of the structure. There is also a peak around 0.8Hz and the second natural frequency of the structure.

The results from this simulation is not physically incorrect. See the discussion in section 14.4.

14.3 Load case $H_S = 3m$, $T_P = 7s$

14.3.1 Wind at hub height = 5.5m/s
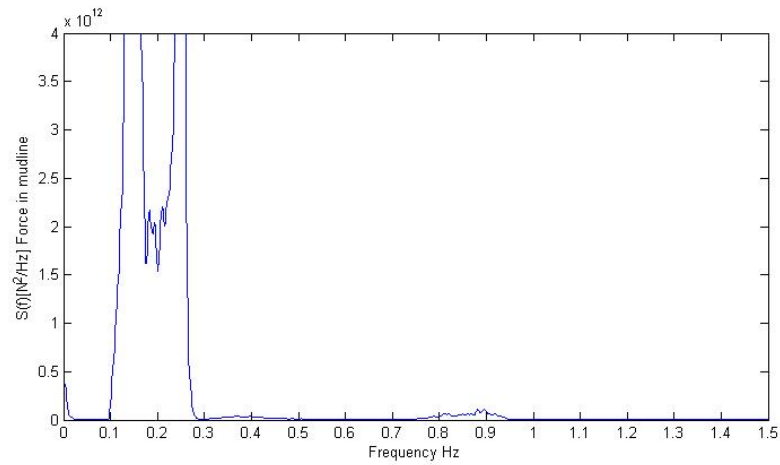

Figure 14.13: Force mudline, HS=3m TP=7s U=5.5m/s
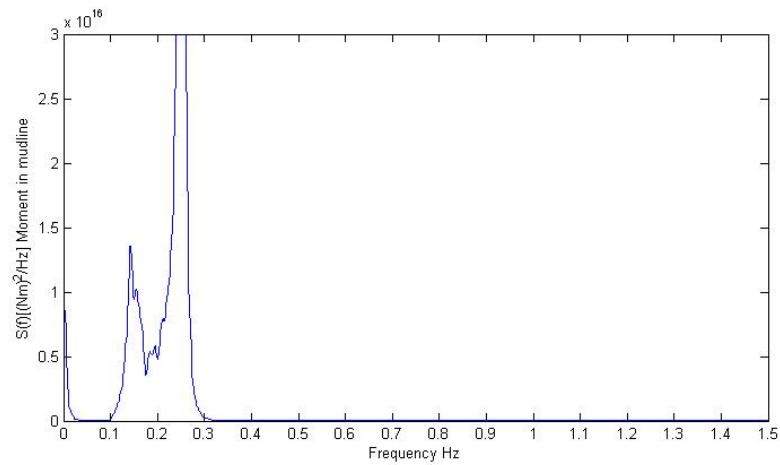
Figure 14.14: Moment mudline, HS=3m TP=7s U=5.5m/s

Figure 14.15: Response mudline, HS=3m TP=7s U=5.5m/s

When the waves have a significant wave height of 3m, we can see a much larger peak in the horizontal force at the wave peak frequency of 0.14Hz compared to $H_S = 1$m and same wind speed. There is still a large contribution at the first natural frequency of the structure which is 0.25 Hz. There is a little energy around the second natural frequency of 0.91 Hz. This is shown in figure 14.13

Figure 14.14 shows the power spectrum of the moment. The peak at the wave peak frequency is larger compared to significant wave height of 1 meters. The peak at the first natural frequency of structure around 0.25Hz is very similar of that for significant wave height of 1m.

The power spectrum of the response is shown in figure 14.15. There is only a peak at the first natural frequency of the structure. The peak is more than twice the height compared to a significant wave height of 1 meters for the same wind speed.

14.3.2 Wind at hub height = 11.1 m/s
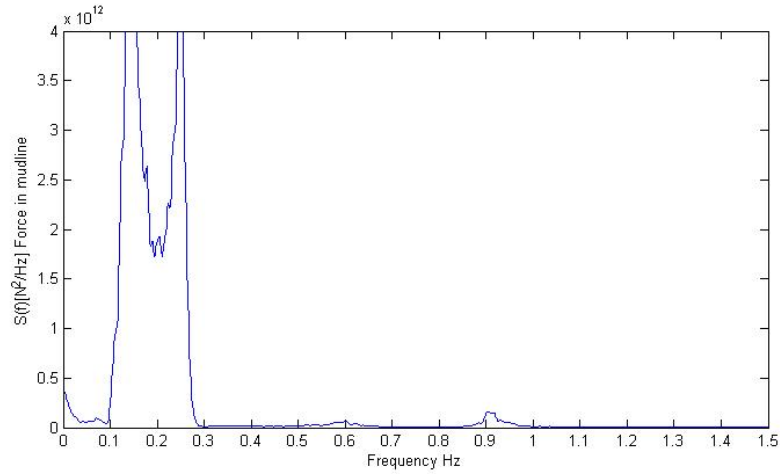
Figure 14.16: Force mudline, HS=3m TP=7s U=11.1m/s
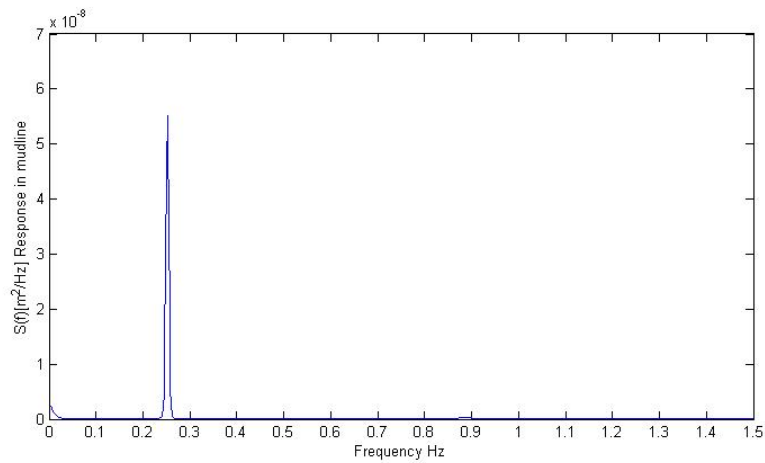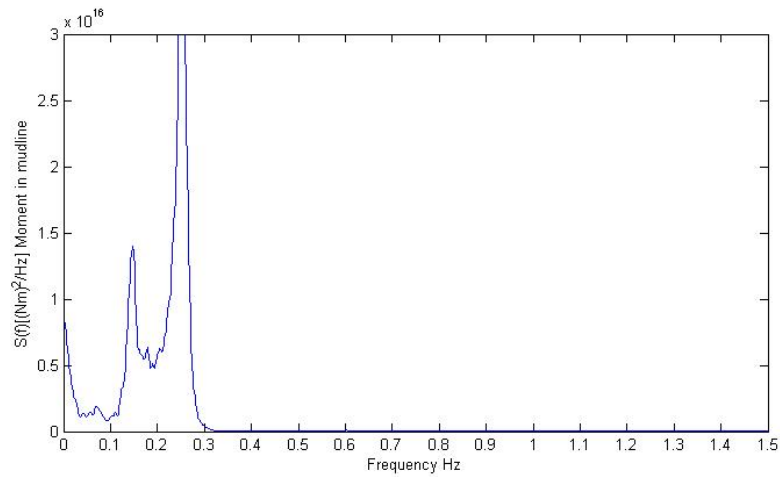

Figure 14.17: Force mudline, HS=3m TP=7s U=11.1m/s
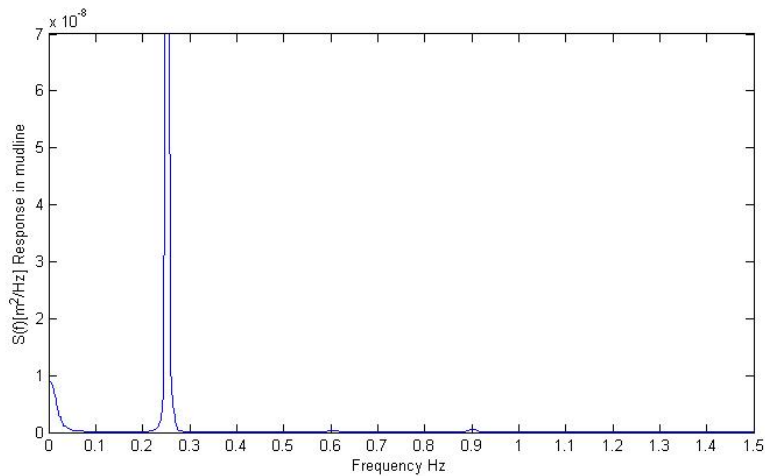
Figure 14.18: Response, HS=3m TP=7s U=11.1m/s

When the wind is around rated speed we have a large peaks at the wave peak frequency of 0.14Hz and the first natural frequency of the structure which is 0.25 Hz. The peak around the second natural frequency of the structure is larger than for a mean wind speed of 5.5m/s for the same wave conditions. This is shown in 14.16.

The shape of the power spectrum for the moment in the mudline is very similar as for a mean wind speed of 5.5m/s. There is more energy in the lower frequencies, while the peaks around the wave peak frequency and the first natural frequency of the structure is almost unchanged. This is shown in figure 14.17

The spectrum for the rotational response in the mudline is shown in figure 14.18. There is a large peak at the first natural frequency of the structure which is larger compared to a mean wind speed of 5.5m/s at hub height.

14.3.3 Wind at hub height = 22 m/s
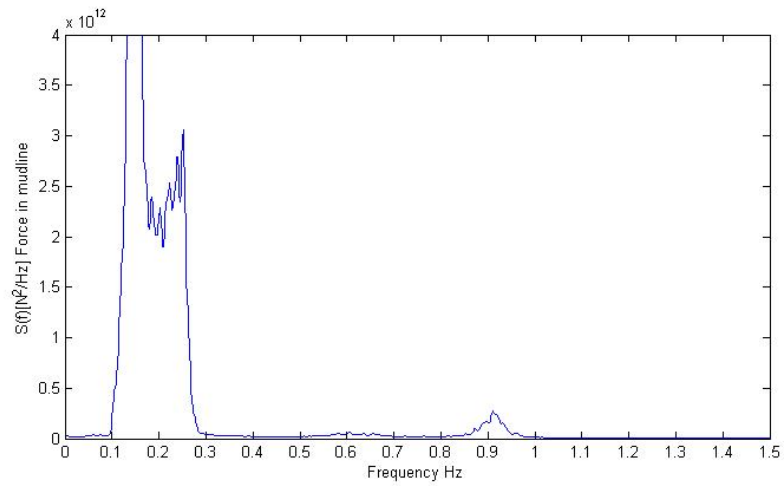
Figure 14.19: Moment mudline, HS=3m TP=3s U=22m/s
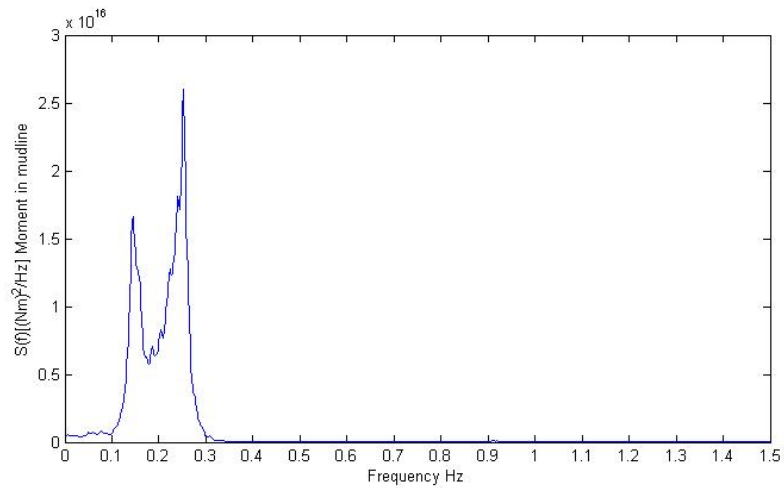
Figure 14.20: Moment mudline, HS=2m TP=6s U=22m/s
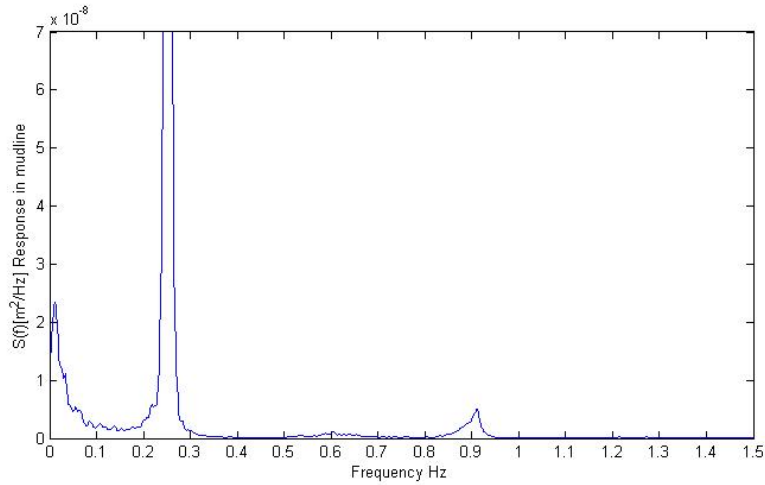
Figure 14.21: Response, HS=2m TP=6s U=22m/s

Figure 14.19 shows the power spectrum of the force in mudline for the given load case. There is a large sharp peak at the wave peak frequency and at the first natural frequency of the structure. The peak at the wave frequency is considerably lower, than for mean wind speed of 5.5 m/s and 11.1m/s at hub height. Also the peak at the first natural frequency is lower.

Figure 14.20 shows the power spectrum of the moment for wind speed of 22m/s and significant wave height of 3m. The peak around the wave peak frequency is similar of that for wind speed of 11.1 m/s while the peak at the first natural frequency of the structure is lower.

The rotational response spectrum is shown in figure 14.21. We can see that the there is more energy in the lower frequencies below 0.1 Hz. The peak around the first natural frequency of the structure is higher and wider compared to lower wind speeds. The peak at the second natural frequency of the structure is higher and have a longer bandwidth compared to a wind speed of 11.1 m/s.

14.4 Discussion

The foundation will experience horizontal forces, moment and response due to the external forces on the turbine and tower.

Low wind speeds
For wind speeds below rated speed there are large peaks around the first natural frequency of the structure for horizontal force, moment and response. When the wave height increases there will be a much larger peak at the peak frequency of the wave. This is clearly shown when comparing a wave height of 1m and 3m. Higher waves will give a higher water particle velocity and acceleration and the wave sweeps a higher length on the tower. This will increase the peak in the power spectrum. Higher waves will also give a larger and wider peak at the first natural frequency of the structure. Larger waves with excitations around the natural frequency will evoke larger resonance behaviour.

Medium wind speeds
When the wind speed is around rated speed which is 11.4 m/s, the shape of the power spectrum is very similar for the force and moment as for wind speeds of 5.5m/s. The response in the foundation is considerably higher at rated speed compared to lower wind speeds. The blades have its highest response at this wind speed, and the response may propagate down to the foundation.

For wind speeds of 14 m/s which is above rated, the peaks fore force and moment around the first natural frequency of the structure is heavily reduced. This applies for wave heights of both 1m and 3m. The peaks at the wave peak frequencies are unchanged. From the thrust curve given in figure 9.2 we can see that the total thrust is reduced for wind speeds above rated. This is due to the pitching of the blades. Lower thrust may contribute to lower the forces in the foundation. The response is similar of that for rated speed.

High wind speeds
For high wind speeds above 14m/s the shape of the force and moment curves in the power spectrum are almost unchanged compared to wind speed of 14m/s. There is a higher peak for the horizontal force around the second natural frequency of the structure. The response in the foundation is at its maximum. For higher wind speeds we can also identify a larger response around the second natural frequency of the structure. It is however very small compared to the response around the first natural frequency. Since the response in the blades are lower for higher wind speeds, it seems like the wake effect of the blades passing the tower gives the largest contribution to response at high wind speeds.

Effects of waves The waves will give forces and moment in the structure around its peak frequency. Some of the waves will have frequencies around the first natural fre-

quency of the structure and contribute to response around the first natural frequency. This is where the force, moment and response has its highest values. Higher waves give higher forces and response.

Effects of wind The wind makes the turbine rotate. The response in the foundation increases with increasing wind velocity. Around the first natural frequency of the structure the response increase dramatically with higher wind speeds. Response around the second natural frequency appears for wind speeds above rated. Since the response in the blades decreases from rated wind speeds and up to wind speeds above rated, it is reasonable to assume that the wake effects from the blades passing the tower is the main contribution to response in the foundation for higher wind speeds.

Response The response in the foundation corresponds to results from previous research. The responses is mainly around the first natural frequency of the structure. There are small contribution around the blade passing frequency of 3P and a little higher contribution around the second natural frequency. This correspond well with the results obtained by VAN DER TEMPEL [26]. Still the effects around the second natural frequency appeared for very high wind speeds in the simulation for this thesis compared to VAN DER TEMPEL, where the effects was observed at wind speed of 8m/s. The simulations performed in FEDEM only revealed very small responses and forces around the blade passing frequency and second natural frequency for low wind speeds. Still there is a need to fully understand the effects of the bending modes of the blades to assess the response on all parts of the structure as discussed by Ibsen et al. [12].

Fatigue considerations The fatigue damage depends on the stresses in the foundation. The total tension depends on the forces and response in the foundation. The forces and moment have very large peaks at the first natural frequency for wind speeds up to rated. For higher wind speeds the peaks of the forces are much lower, but the response is much higher. The first natural frequency is very important for fatigue considerations.

For the second natural frequency of the structure we only experience response and horizontal forces at high wind speeds. Even though the peak at the second natural frequency is considerably lower than around the first, it occurs at a much higher frequency. Fatigue damage depends on the number of cycles of stresses. Even though the responses are much lower they will have a much higher number of cycles and may contribute to decrease the fatigue life of the foundation.

Errors in simulation For the load case $H_S = 2$m, $T_P = 6$s and $U_{hub} = 11.1$m/s the simulation gives results which seems wrong. For forces and moments there are large peaks around 2P and 4P frequency corresponding to 0.4Hz and 0.8Hz. For a two bladed turbine this gives physical meaning as 2P and 4P is a multiple of 2. For a three bladed turbine where the response is dependent on the blades passing the tower there should not be contribution around 2P and 4P. The reasons for the results are unknown. Most likely the control system for the turbine may cause an error around rated speed. There

may also be something wrong with the model. The results may give reason to doubt the results from the other simulations. However, the other results give physical meaning.

15 Conclusion

Sensitivity of second bending mode with increasing rotor diameter
Larger turbines will decrease the eigen-frequencies of the structure. Both the first fore-aft and side-to-side bending mode and the second fore-aft and side-to-side bending mode will have lower eigen-frequencies. This is due to the combination of higher top mass, further distance from the rotor to the tower and longer tower.

Blade forces and response
Without the effects of turbulence the blades will experience a load and response peak at the rotational frequency of the turbine. When turbulence is introduced, the blades will experience a load peaks and response peaks at the rotational frequency and the its higher harmonics. The load and response peaks are highly correlated along the blade in turbulent wind. For larger rotors the forces and responses of the blades will be even greater since the forces are correlated along the blade.

Forces and response in the foundation
Both waves and wind will influence the forces and response in the structure. Higher waves will increase the forces and moment in the foundation at the wave peak frequency. Also resonance behaviour is triggered around the first natural frequency of the structure. A very soft structure is not recommended as this will have natural frequency closer to the wave frequencies. Increasing wind speed will heavily reduce the forces and moments around the natural frequency of the structure. Pitching of the blades will reduce the thrust force, and hence reduce the horizontal force and moment in the foundation. For high wind speeds, effects from the rotor dominates the response in the foundation. The wake effects from the blades passing the tower increases with the wind speed. For high wind speeds there will be horizontal force and response around the second natural frequency.

Fatigue consideration
For large wind turbines there will be a response peak around the second bending mode of the structure. The peak around the first natural frequency will contribute to fatigue due to the high peak. Response around the second bending mode may also contribute. The peak is much smaller, but appears at a higher frequency which means more cycles of stresses in the foundation.

16 Further work

In the course of working with this thesis, there have been identified issues that needs further work.

There were uncertainties in one simulation where there were results that do not fit with the physics of an offshore wind turbine. Verification of the model or the control system needs to be done to fully trust the simulations that where performed.

The dynamic response of an offshore wind turbine is a very complex system with a lot of interaction frequencies. To fully understand vibration analysis, more work have to be done in understanding the mode shapes end eigen-frequencies of the blades. Also more effort in the rotational sampling need to be conducted to fully understand the forces and responses of the blades in turbulent wind. The effects of the blade passing frequency needs to be investigated further. The wake effects of the blades passing the tower and tower shadowing have to be understood to understand the dynamic response of the structure.

Investigation on the sensitivity of eigen-frequencies with increasing rotor where performed under certain assumptions and manipulation of the model. An actual model of large blades have to be implemented to calculate the eigen-frequencies. Especially if one considers the response in the blades. Also a larger turbine should be used in simulations to investigate properly the effects of larger turbines.

References

[1] Fedem user's guide, release 7.0.3. 2013.

[2] Povl Brøndsted, Hans Lilholt, and Aage Lystrup. Composite materials for wind power turbine blades. *Annu. Rev. Mater. Res.*, 35:505–538, 2005.

[3] BH Bulder, HB Hendriks, PJ van Langen, C Lindenburg, H Snel, P Bauer, H Polinder, R van Rooij, H Subroto, and MB Zaayer. The icorass feasibility study. *Wind Energy*, 2012:2011, 2013.

[4] Tony Burton, Nick Jenkins, David Sharpe, and Ervin Bossanyi. *Wind energy handbook*. John Wiley & Sons, 2011.

[5] Subrata Kumar Chakrabarti. *Hydrodynamics of offshore structures*. WIT press, 1987.

[6] Johan Driesen, Thierry Van Craenenbroeck, Roland Reekmans, and Daniel Van Dommelen. Analysing time-varying power system harmonics using wavelet transform. In *Instrumentation and Measurement Technology Conference, 1996. IMTC-96. Conference Proceedings. Quality Measurements: The Indispensable Bridge between Theory and Reality., IEEE*, volume 1, pages 474–479. IEEE, 1996.

[7] Odd Faltinsen. *Sea loads on ships and offshore structures*, volume 1. Cambridge university press, 1993.

[8] Leon L Freris. *Wind energy conversion systems*. Prentice Hall, 1990.

[9] Klaus Hasselmann, TP Barnett, E Bouws, H Carlson, DE Cartwright, K Enke, JA Ewing, H Gienapp, DE Hasselmann, P Kruseman, et al. Measurements of wind-wave growth and swell decay during the joint north sea wave project (jonswap). 1973.

[10] Guy T Houlsby and Byron W Byrne. Suction caisson foundations for offshore wind turbines and anemometer masts. *Wind Engineering*, 24(4):249–255, 2000.

[11] Jörg Höyland. Challenges for large wind turbine blades. 2010.

[12] Lars Bo Ibsen and Morten Liingaard. Output-only modal analysis used on new foundation concept for offshore wind turbine. 2005.

[13] BJ Jonkman and L Kilcher. Turbsim user's guide: Version 1.06. 00. *NREL/TP-xxx-xxxx (Draft Version), Golden, CO: National Renewable Energy Laboratory*, 2012.

[14] Jason Mark Jonkman, Sandy Butterfield, Walter Musial, and G Scott. *Definition of a 5-MW reference wind turbine for offshore system development*. National Renewable Energy Laboratory Golden, CO, 2009.

[15] Erwin Kreyszig. *Advanced engineering mathematics*. John Wiley & Sons, 2007.

[16] James F Manwell, Jon G McGowan, and Anthony L Rogers. *Wind Energy Explaned.* Wiley Online Library, 2010.

[17] Roux Martin. Wind turbines, types, economics and development. 2010.

[18] David-P Molenaar and Sjoerd Dijkstra. Modeling the structural dynamics of flexible wind turbines. In *EWEC-CONFERENCE-*, pages 234–237, 1999.

[19] Willard J. Pierson and Lionel Moskowitz. A proposed spectral form for fully developed wind seas based on the similarity theory of s. a. kitaigorodskii. *Journal of Geophysical Research*, 69(24):5181–5190, 1964.

[20] Wojciech Popko, Fabian Vorpahl, Adam Zuga, Martin Kohlmeier, Jason Jonkman, Amy Robertson, Torben J Larsen, Anders Yde, Kristian Sætertrø, Knut M Okstad, et al. Offshore code comparison collaboration continuation (oc4), phase i–results of coupled simulations of an offshore wind turbine with jacket support structure. In *22nd International Society of Offshore and Polar Engineers Conference. Rhodes, Greece*, 2012.

[21] Magnar Reistad, Øyvind Breivik, Hilde Haakenstad, Ole Johan Aarnes, Birgitte R Furevik, and Jean-Raymond Bidlot. A high-resolution hindcast of wind and waves for the north sea, the norwegian sea, and the barents sea. *Journal of Geophysical Research: Oceans (1978–2012)*, 116(C5), 2011.

[22] D Salzmann and J Van der Tempel. Aerodynamic damping in the design of support structures for offshore wind turbines. In *Paper of the Copenhagen Offshore Conference*, 2005.

[23] Paul Stansell. Distributions of extreme wave, crest and trough heights measured in the north sea. *Ocean Engineering*, 32(8):1015–1036, 2005.

[24] D Tcherniak, Shashank Chauhan, and Morten Hartvig Hansen. Applicability limits of operational modal analysis to operational wind turbines. In *Structural Dynamics and Renewable Energy, Volume 1*, pages 317–327. Springer, 2011.

[25] T Tjelta. Geotechnical experience from the installation of the europipe jacket with bucket foundations. In *Offshore Technology Conference*, 1995.

[26] Jan Van Der Tempel. Design of support structures for offshore wind turbines. 2006.

[27] Det Norske Veritas. Dnv-rp-c205 environmental conditions and environmental loads. *Norw ay: DetNorskeVeritas*, 2010.

A   Attachment

- **Poster.pdf:** Poster presentation of thesis for the Master Thesis Poster

- **powerSpectrum.m:** Matlab script for transforming time series into power density spectrum